

Review

# Quantifying Hydrothermal Alteration: A Review of Methods

Lucie Mathieu 

Centre D'études sur les Ressources Minérales (CERM), Département des Sciences Appliquées, Université du Québec à Chicoutimi (UQAC), 555 boul. De L'université, Chicoutimi, QC G7H 2B1, Canada; lucie1.mathieu@uqac.ca; Tel.: +1-418-545-5011 (ext. 2538)

Received: 28 May 2018; Accepted: 29 June 2018; Published: 3 July 2018



**Abstract:** Hydrothermal alteration is proximal to many base and precious metal deposits, and its products can provide insights into the characteristics of hydrothermal systems. To be useful to exploration geologists and researchers, however, alteration needs to be typified and quantified. Alteration type informs on mineralising style (e.g., have we found a porphyry or a volcanogenic massive sulphide deposit?), while quantification of its intensity helps position a sample within the system (e.g., how close are we to the main economic deposit?). Numerous methods—all having their specific advantages and disadvantages—are dedicated to the characterisation of alteration. As alteration is a process that induces chemical and mineralogical changes in rocks, it can be studied using petrological (e.g., mineral recognition in thin sections, mineral chemistry), mineralogical (e.g., alteration indices that use normative minerals), and chemical (e.g., mass balance calculations) approaches. This short review provides an overview of the methods useful to researchers and that are also applicable in an exploration context.

**Keywords:** hydrothermal alteration; mass balance; alteration indices; normative calculation; porphyry

## 1. Introduction

Hydrothermal alteration is proximal to many precious and base metal deposits, such as, in Archean greenstone belts, volcanogenic massive sulphide (VMS) deposits, porphyries as well as intrusion-related and orogenic gold mineralisation. These deposits are the result of hydrothermal to magmato-hydrothermal systems encompassed by thin (centimetres) to extensive (hundreds of kilometres) alteration halos [1–3]. Halos are important indicators to mineral exploration companies, which are continually searching for reliable and easy-to-use approaches for finding mineralisation sites.

Alteration is an open system process that results in chemical and mineralogical changes in a rock. A similar definition applies to metamorphism. However, the chemical changes induced by metamorphism are generally less intense than those observed within altered rocks. Distinction between these processes is subtle where deposits are formed by metamorphic fluids, such as orogenic gold deposits [4]. Weathering is another process that induces extreme chemical and mineralogical changes, but in contrast to hydrothermal alteration, it is restricted to superficial rocks and involves low-temperature fluids.

Hydrothermal alteration is also generally distinguished from changes induced in rocks by magmatic fluids (e.g., feniitisation [5]). However, again the distinction is subtle, as magmatic fluids are involved in several mineralising processes, such as porphyries, syenite-associated deposits, and some VMS [6–8]. Another term often encountered is “metasomatism” that is defined, for metamorphic rocks, as follows [9]:

*“A metamorphic process by which the chemical composition of a rock or rock portion is altered in a pervasive manner and which involves the introduction and/or removal of chemical components as a*

*result of the interaction of the rock with aqueous fluids (solutions). During metasomatism the rock remains in a solid state."*

Metasomatism can be observed in any metamorphic context; it may refer to fluid-induced modifications of mantle rocks [10], and is also synonymous with alteration [11], even if the terms metasomatism and alteration have been used to designate chemical and mineralogical changes, respectively [12]. This review focuses on hydrothermal alteration—chemical and mineralogical changes induced by moderate to high temperature mineralising fluids (300–350 °C for orogenic gold deposits, for example [4])—that interact with upper crustal rocks (surficial rocks for VMS systems through to the greenschist-amphibolite facies for orogenic gold deposits [4,13]).

The products of alteration provide insights into the characteristics of hydrothermal systems, while also being useful vectors toward mineralisation. In this review, hydrothermal alteration is viewed from an exploration perspective. Metals tend to concentrate in the most intensely altered rocks; sites where the greatest amount of fluids (high fluid/rock ratio) having peculiar characteristics (such as highest temperature, lowest pH) interacted with crustal rocks. However, to be useful for exploration, alteration must be recognised, typified, but, most importantly, quantified.

This review concentrates on methods that can be easily applied in an exploration context [14,15] to quantify the intensity of an alteration process. Numerous methods, including alteration indices, norms, and mass balance calculations, can be used to quantify alteration [16–18]. Each method has its specific advantages and requirements, and the challenge is selecting the appropriate method for a given situation. This review aims to provide an overview of these methods and to compare their performance and applicability within multiple contexts.

Alteration indices and mass balance calculations are the main approaches addressed in this review. Mass balance calculations have two main requirements—identifying immobile elements and a precursor [18]. These aspects will be discussed in detail. An immobile element is, by definition, immobile during the hydrothermal event being investigated. In metamorphic geology, a protolith designates a rock whose mineral assemblages were modified to form a metamorphic rock. By analogy, a precursor is a fresh rock that has interacted with a hydrothermal fluid to form an altered rock.

An additional constraint for exploration geologists is the need to rapidly quantify alteration, given that time-consuming petrographic observations are not always possible. Furthermore, existing data sets may lack some chemical analyses, such as trace elements or ferrous and ferric iron analyses, useful for identifying alteration. Petrographic descriptions [19] and methods [20,21] that apply to such often missing data are thus not reviewed. Instead, this short review focuses on methods applicable to incomplete whole-rock chemical data. Each method is illustrated using chemical analyses compiled from the scientific literature.

## 2. Theoretical Considerations

This section summarises the basic notions necessary for quantifying alteration.

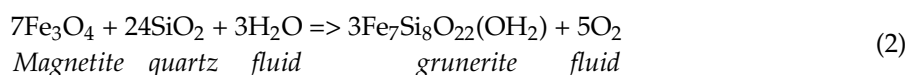
### 2.1. Alteration Types

This section summarises the basic concepts of alteration processes to help interpret the calculations described hereafter. It is also a good practice to list the expected alteration types for a given context to facilitate the interpretation of alteration indices and mass balance calculations.

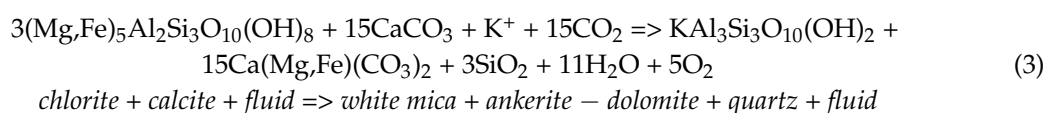
Sulphidation produces sulphides from fluids generally carrying S and metals. If these elements combine with the Fe of the host rock, then only S and the metal gains are measured (Table 1). Lithological controls are expected in Fe-enriched contexts (e.g., Fe-formations of Meliadine, an orogenic gold district) [22].

Silicification is expressed in the field as quartz veins and stockwork or as “silica flooding” (i.e., pervasive silicification). Silicification is common, as Si is an abundant and soluble element (Table 1). An addition of Si to a rock produces either quartz (Equation (1)) or other minerals in; for example, iron formations (Equation (2)) [23]. However, silicification and quartz proportions

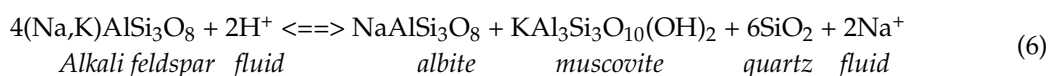
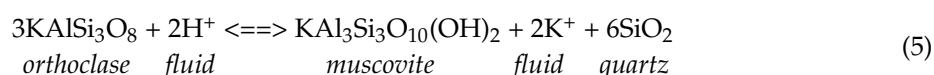
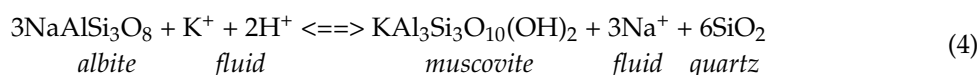
correlate poorly, because magmatic, detritic, and metamorphic quartz are abundant, and because quartz is a sub-product of several alteration reactions (e.g., Equations (3)–(6)) [23]. It is thus best to use mass balance calculations instead of petrological observations to quantify silicification.



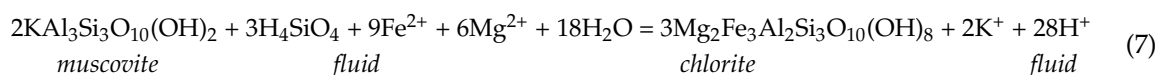
Carbonatisation produces carbonates and corresponds to a CO<sub>2</sub> gain (Table 1). To remain in a rock, C must combine with Ca, Mg, and/or Fe, which are either brought by the fluid or are taken from the constituent minerals of the fresh rock. In the latter case, maximum carbonate proportion is dependent on the composition of the precursor. Furthermore, if C combines with the Ca of plagioclase, then paragonite and quartz by-products form, while the destabilisation of other minerals—alkali feldspar and clinopyroxene—may form muscovite and chlorite [15]. Thus, quantifying the intensity of carbonatisation and distinguishing phyllosilicate by-products from those related to sericitisation and chloritisation processes is not straightforward. Characterisation of the carbonate phases is also pertinent, as Ca- and Fe-Mg-carbonates are observed in weakly and intensely altered rocks, respectively (Equation 3, modified from Colvine [23]).



Sericitisation is an acidic alteration that produces white mica—mostly thin muscovite (sericitic texture). A commonly held belief is that sericitisation is systematically accompanied by a K-gain (Equation (4)). However, sericitisation destabilises feldspar and may induce K-loss (Equation (5)) [24,25]. Depending on the precursor, by-products such as albite and quartz may be produced (Equation (6)) [23] and plagioclase destruction may produce paragonite. Sericitisation generally results in Ca- and Na-losses, accompanied by a K-gain or loss (Table 1).



Chloritisation corresponds to gains of Fe and Mg and produces chlorite (Table 1). As with carbonatisation, Fe- and Mg-gains induce mineralogical changes as these elements combine with Si—transported or not by the fluid—and Al (an immobile element) to form chlorite. This process is well documented in VMS systems, where chloritisation destabilises the muscovite produced by a preceding sericitisation process, induces K-loss, and increases the acidity of the fluid (Equation (7)) [26]. In addition, a zonation is generally observed, with Mg-chlorite being more distal from the core of the system than Fe-chlorite [27]. Chloritised rocks display Fe- and/or Mg-gains and Ca-, Na-, and/or K-losses.



Propylitic alteration is a common distal and weak alteration observed in porphyry systems. This process produces calcite, chlorite, epidote, and albite (Table 1), which are greenschist facies minerals observed in unaltered rocks (calcite excepted). Propylitic alteration corresponds to carbonatisation combined with hydration occurring at moderate temperatures.

Albitisation and K-feldspar alterations correspond to Na- and K-gains, respectively (Table 1). The added Na and K generally combine with the Al of pre-alteration feldspars to form alteration feldspars, and these replacement reactions are not always easy to recognise [15]. They may induce Na- or K-gain accompanied by Ca-, Na-, and/or K-losses. Additional losses of Fe, Mg, and possibly Si may be necessary to form albitites [28].

**Table 1.** Alteration types and associated chemical changes and alteration minerals.

	Mass Changes	Examples of Assemblages
Sulphidation	+S, +metals	Any minerals + sulphides
Silicification	+Si	Any minerals + quartz
Carbonatisation	+C, (+Ca)	Carbonates ± quartz-white mica-chlorite <sup>1</sup> Talc + chlorite + carbonate <sup>2</sup>
Sericitisation	+K or -K, -Na, -Ca, +H	White mica + quartz + pyrite <sup>3</sup>
Chloritisation	+Fe, +Mg, +H -Na, -Ca, -K	Chlorite + pyrite + white mica ± quartz <sup>1</sup>
Propylitisation	+H, +C	Epidote + chlorite + albite ± carbonate <sup>3</sup>
K-feldspar alteration	+K, -Na	K-feldspar + biotite + quartz <sup>3</sup>
Albitisation	+Na, -K	Albite + hornblende ± biotite-quartz <sup>4</sup>

<sup>1</sup> Example from a VMS system [19]; <sup>2</sup> Example from altered komatiites in a orogenic gold system [16]; <sup>3</sup> Key minerals compiled by Gifkins et al. [19]; <sup>4</sup> Example from a porphyry system [28].

## 2.2. Altered Rocks, Analysis, and Sampling

This review focuses on methods applicable to chemical analyses of whole-rock samples. Good quality analyses are now routinely performed on behalf of mining companies, using methods such as X-ray fluorescence spectrometry (XRF), inductively coupled plasma atomic emission spectrometry (ICP-AES) or mass spectrometry (ICP-MS), and occasionally neutron activation analysis (NAA) (for a discussion on these methods, see Gifkins et al. [19]). Sampling, however, is not as straightforward and depends on the distribution of the alteration minerals.

The changes induced in a rock by an hydrothermal fluid can present a wide range of geometries and textures in the field [19]. For example, infilling may correspond to the development of alteration minerals in any available open space (e.g., pores, fractures). In a porous rock, pore-filling [29] may form evenly distributed minerals. However, this process may also form veins, veinlets, and stockworks [6], and the sampling of a representative number of veins can be challenging. In addition, the elements discharged by the fluid interact variably with the hosting material, and the intensity of an alteration process (e.g., amount of mass gained) can depend on the composition (carbonatisation) or rheology (quartz veins) of the precursor. Each alteration style must be sampled representatively.

Alteration may also preferentially affect particular phases; for example, sericitisation affects feldspars, martitisation affects magnetite, and carbonatisation tends to affect Ca-bearing phases [23]. Replacement and leaching are strongly dependent on the composition of the precursor. Consequently, relating mass changes or the proportion of alteration minerals to the intensity of alteration is not straightforward. Sampling, on the other hand, is easy if the alteration minerals are evenly distributed within the rock and challenging if the replaced minerals are large or unevenly distributed. The sampling of vein-forming minerals is particularly difficult, as veins are either avoided or targeted by sampling procedures. In such situations, larger samples may be required.

There are no easy solutions to these sampling issues [30,31], and a possible strategy is to select evenly distributed samples (e.g., 20-cm-long samples located every 3 m along a drilled core) irrespective of their alteration and ore mineral contents. In addition, alteration minerals may have been produced by separate hydrothermal events, but only bulk changes are quantified by the methods presented hereafter. Precise investigations of individual events require dedicated sampling or sample preparation, such as excising veins prior to analysis. This is generally unrealistic in an exploration context. Careful interpretation of bulk changes may, however, provide insights into complex hydrothermal events (e.g., Phelps–Dodge VMS, Section 5.5).

### 3. Presentation of the Data Sets

In the following sections, the presented methods are illustrated using a series of existing data sets.

A fresh volcanic rocks data set containing four entries (Table 2) is used to monitor the results. These data correspond to the mean values of fresh volcanic rocks, for rhyolite, dacite, andesite, and calc-alkaline to tholeiitic basalt, of the pre-compiled files of the GEOROC database (<http://georoc.mpch-mainz.gwdg.de/georoc/>) [32].

**Table 2.** Mean major and trace elements content of volcanic rocks of the GEOROC database, including values for several alteration indices and mass balance calculations (see the text for the definition of these indices and calculations).

	Rhyolite	Dacite	Andesite	Basalt
Samples (n)	3423	3753	12,315	1360
SiO <sub>2</sub> (wt %)	73.28	65.90	57.26	51.05
TiO <sub>2</sub>	0.36	0.60	0.93	1.33
Al <sub>2</sub> O <sub>3</sub>	13.24	15.72	16.67	15.46
Fe <sub>2</sub> O <sub>3</sub> <sup>T</sup>	2.71	4.75	8.58	11.73
MgO	0.49	1.70	4.08	6.41
MnO	0.07	0.09	0.14	0.18
CaO	1.32	3.86	7.11	9.64
Na <sub>2</sub> O	3.51	3.87	3.43	2.56
K <sub>2</sub> O	4.06	2.62	1.54	0.79
P <sub>2</sub> O <sub>5</sub>	0.07	0.18	0.24	0.21
LOI	1.25	1.24	1.00	1.06
Cr (ppm)	18.29	36.27	90.68	191.54
Zr	297.85	174.84	137.55	109.75
Y	44.64	22.70	23.41	25.64
Fe <sub>2</sub> O <sub>3</sub> /Fe <sub>2</sub> O <sub>3</sub> <sup>T1</sup>	0.40	0.35	0.30	0.20
FeO	1.46	2.78	5.40	8.45
Fe <sub>2</sub> O <sub>3</sub>	1.08	1.66	2.57	2.35
AI	48.51	35.85	34.78	37.11
CCPI	37.75	43.59	52.82	58.17
ALT_CHLO	3.59	8.78	10.36	10.68
ALT_MUSCV	5.61	0.69	0	0
MB_CaO <sup>2</sup>	−0.01	−0.34	−0.72	−0.23
MB_Fe <sub>2</sub> O <sub>3</sub> <sup>T</sup>	−0.26	0.12	0.34	−0.07
MB_K <sub>2</sub> O	0.78	0.04	−0.08	0.07
MB_MgO	0.06	−0.17	−0.40	−0.29
MB_Na <sub>2</sub> O	−0.42	0.01	−0.10	−0.18
MB_SiO <sub>2</sub>	8.68	3.04	−1.35	−0.84

<sup>1</sup> Factor used to model the FeO and Fe<sub>2</sub>O<sub>3</sub> values. <sup>2</sup> MB stands for mass balance calculation (modelled precursor method, see text for explanation), in g. per 100 g of precursor.

The Hongtoushan data set contains 51 samples from Liaoning Province, NE China, from a VMS metamorphosed to the conditions of the upper amphibolite facies [33]. The sampled rocks are basalts to rhyolites and are classified as altered or unaltered rocks on the basis of petrological observations [33].

The samples were analysed by XRF and ICP-MS, and alteration indices, mass changes, and stable isotopes indicate that these rocks have mostly been chloritised [33].

The Chibougamau data set contains 261 anorthosite and gabbro samples that have been analysed by XRF, ICP-MS, ICP-AES, and NAA. These samples are from the Central Camp, a Cu-Au porphyry mineralisation located in the Abitibi Subprovince, Canada. The analyses were extracted from the Ministère de l'Énergie et des Ressources Naturelles (MERN) database (<http://sigeom.mines.gouv.qc.ca>). The Central Camp deposits have been metamorphosed to greenschist facies conditions, and the main alteration minerals are sulphides, quartz, carbonate (siderite, ankerite), white mica, chlorite, and chloritoid [34–38]. FeO and Fe<sub>2</sub>O<sub>3</sub> values are available for 24 samples that have Fe<sub>2</sub>O<sub>3</sub>/Fe<sub>2</sub>O<sub>3</sub><sup>T</sup> ratios of about 0.2 (median = 0.208, Q1 = 0.158, Q3 = 0.254). The particularity of this data set is that it contains samples having precursors that grade from gabbro to anorthosite. Furthermore, most samples lack trace element analyses and petrographic observations. As such, most of the techniques described hereafter would normally provide imprecise results.

The Arunta data set contains 30 samples—all having undergone unspecified analytical techniques—from a small metamorphosed VMS deposit within the Arunta block, Australia [39]. The observed rocks are mafic granulites, moderately migmatized quartzofeldspathic gneisses, and cordierite quartzites, whose photoliths are interpreted as basalts, unaltered felsic igneous rocks, and their chloritised equivalents, respectively [39]. The Fe<sub>2</sub>O<sub>3</sub>/Fe<sub>2</sub>O<sub>3</sub><sup>T</sup> ratio is about 0.2 (median = 0.221, Q1 = 0.108, Q3 = 0.389) for 24 of 30 samples.

The Roberto data set contains 32 samples from the James Bay area, Québec, that have been analysed by XRF and ICP [40,41]. Roberto is a gold deposit located in turbiditic metagreywacke and paragneiss metamorphosed to the amphibolite facies. The mineralisation is spatially associated with calc-silicate- and tourmaline-bearing quartz veins, and metasomatic replacement zones (Ca- and K-gains) [40]. The area records a long succession of metamorphic and magmatic events, and the deposit was deformed and metamorphosed to the amphibolite facies [41,42].

The La Grande Sud data set contains 47 tonalite samples from the James Bay area, Québec [43]. The samples were analysed by XRF, NAA, and ICP-AES. La Grande Sud is a small (0.6 × 1.5 km) tonalite intrusion located in Archean supracrustal rocks in the La Grande Subprovince. The intrusion contains several Au-Cu showings (disseminated sulphides) associated with breccia, quartz, and carbonate veins, potassic and propylitic assemblages, sericitisation, and carbonatisation [43,44]. This synvolcanic porphyry-like mineralisation has been metamorphosed to the conditions of the greenschist facies, deformed, and possibly overprinted by late hydrothermal events [43,44]. Mercier-Langevin [43] studied the tonalite samples and identified Sample #19449 as being least-altered, as petrological investigations showed this sample as containing the least amount of white mica, chlorite, and carbonate.

The Phelps–Dodge data set contains 22 samples of XRF-analysed altered rhyodacite from an Archean VMS within the Matagami camp, Abitibi Subprovince, Québec [45]. These rocks have undergone silicification and chloritisation accompanied by feldspar destruction, followed by Si-leaching [45]. The analysed immobile elements are Zr, Y, Nb, Ti, and Al. These elements are well correlated, indicating that they are immobile, and that the system has a single precursor [45]. Sample #18 is least-altered according to petrological observations [45]. A particularity of this data set is that Na<sub>2</sub>O, K<sub>2</sub>O, and CaO are summed, preventing the calculation of alteration indices. However, because a precursor and immobile elements have been identified, this data set remains suitable for mass balance calculations.

#### 4. Alteration Indices

Alteration indices require only the analysis of major elements and can thus be applied to most data sets. They are dimensionless numbers comprised between 0 (fresh rocks) and 1 or 100% (intensely altered rock). Alteration indices consider mineralogical constraints and thus have the advantage of

relating petrological observations to chemical analyses. This section summarises a series of alteration indices calculated from major elements and normative minerals.

#### 4.1. Major Element Ratios

Alteration indices can correspond to ratios of selected mobile major elements, which are representative of an alteration mineral of interest or of a primary mineral destabilised by the alteration process. These indices are easy to calculate and are popular among exploration geologists. Many alteration indices have been proposed over the years, such as the Ishikawa alteration index (AI) (Equation (8)) [46] and the chlorite–carbonate–pyrite index (CCPI) (Equation (9)) [26]:

$$AI = 100 \times (K_2O + MgO)/(K_2O + MgO + Na_2O + CaO) \quad (8)$$

$$CCPI = 100 \times (FeO^T + MgO)/(FeO^T + MgO + Na_2O + CaO) \quad (9)$$

Most indices are designed to quantify specific alteration types; for example, AI is dedicated to sericitisation and chloritisation [46]. However, when we calculate AI and CCPI using the mean values of fresh volcanic rocks, we observe magmatic fractionation-related variations (Table 2). Alteration indices rarely take a constant value (0 or else) when calculated in fresh rocks; they are dependent of the nature of the precursor. Interpreting alteration indices thus requires insights into the composition of the precursors (Table 3).

The value of an alteration index such as AI can be modified by sericitisation (with or without K-gains) and chloritisation, but also by Ca-metasomatism. On the other hand, the albite saturation index (Na/Al molar [16]) may be modified by albitisation, K-feldspar alteration, and feldspar destruction that accompanies sericitisation and chloritisation. Interpreting alteration indices is thus challenging. Using binary diagrams can help with interpretation, as the values that the index typically generates in fresh rocks can be represented by fields having complex shapes [47]. Other binary diagrams use two indices and allow for a larger number of alteration trends to be displayed; for example, the alteration box plot that is designed for VMS systems [26]. On the alteration box plot, chloritisation causes samples to be displaced from the centre of the diagram toward its upper right-hand part, sericitisation induces displacement toward the right, and so on [26].

To illustrate this method, alteration indices are calculated for the 51 samples of the Hongtoushan VMS [33]. This metamorphosed VMS has altered and unaltered rocks that still display distinctive chemistries despite the high grade metamorphic event (Figure 1a). The bulk-rock chemical changes induced by metamorphism are likely limited compared to the changes induced by the preceding hydrothermal event, and insights into the alteration process can still be gained from the analysis of major elements [14]. As most samples are positioned close to the upper right-hand corner of the diagram, chloritisation is likely intense (Figure 1b).

The Hongtoushan data set is ideal for the calculation of alteration indices, as there are well-documented precursors and only chloritisation is reported. Areas having poorly documented precursors and alteration processes, and/or overlapping hydrothermal systems may not be suitable for this method. Apart from these restrictions, alteration indices remain a useful and easy-to-use approach that can be applied to most data sets encountered within an exploration context (Table 3).

**Table 3.** Characteristics of alteration indices.

Method—Alteration Indices	
<b>Advantage</b>	Easy to calculate
<b>Disadvantage</b>	Strongly sensitive to the composition of the precursors
<b>Requirements</b>	Whole-rock chemical analyses (major elements), known precursors
<b>Recommendation</b>	To be used only in well-documented areas

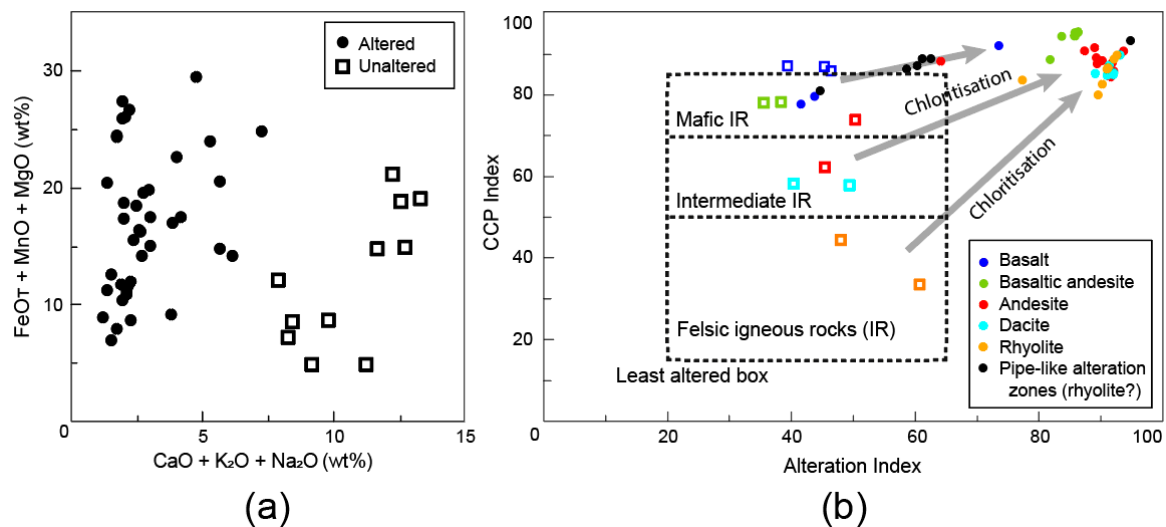


**Figure 1.** Diagrams displaying 51 samples from the Hongtoushan VMS [33]. (a) Binary diagram displaying the main chemical differences between the altered and unaltered rocks; and (b) alteration box plot [26] with chloritisation trends. The fields for least-altered felsic to mafic rocks are from Gifkins et al. [19].

#### 4.2. Normative Mineral Ratios

Normative calculations are also used to verify or replace, in part, petrological observations. Several normative calculations have been proposed [48–50], such as the Normat method [17] that is designed for VMS systems. Normat provides accurate estimates of the proportions of carbonates, even when CO<sub>2</sub> has not been analysed. The normative estimate of CO<sub>2</sub> has been integrated to other norms, such as the CONSONORM\_LG and CONSONORM\_HG methods [51,52] that are designed for low-grade and high-grade metamorphic rocks, respectively. These normative calculations are intended for a wide range of P-T conditions, rock types, and mineralisation contexts.

Normative calculations are run on major elements (including FeO and Fe<sub>2</sub>O<sub>3</sub>). These values can be analysed or estimated [53,54] (Table 4). The calculations are described in greater detail in the literature [17,51,52]. The alteration indices are intended for specific alteration types; for example, the ALT\_MUSCV (Equation (10)) and ALT\_CHLO (Equation (11)) indices of the CONSONORM\_LG method [51] quantify sericitisation and chloritisation, respectively.

$$\text{ALT\_MUSCV} = 100 \times \text{muscovite} / (\text{sum of all minerals except quartz and sulphides}) \quad (10)$$

$$\text{ALT\_CHLO} = 100 \times \text{chlorite} / (\text{sum of all minerals except quartz and sulphides}) \quad (11)$$

These indices are relatively insensitive to the composition of the precursors [51]. They take moderate values (<10%) in fresh magmatic rocks, as demonstrated by calculating the 2SV350 model (representing 350 °C and 2.5 kbar) of the CONSONORM\_LG method on the fresh rocks of the GEOROC database (Table 2). These indices are therefore ideal in poorly documented contexts. In cases of metamorphism, such as VMS metamorphosed to a high-grade condition [14], it is assumed that chemical changes induced by alteration processes are much greater than metamorphism-related modifications. This assumption is reasonable, as long as the investigated alteration process does not implicate a volatile element other than H<sub>2</sub>O (e.g., carbonatisation), and as long as migmatites are rare to absent.

In the lowest-grade rocks, in which de-volatilisation is limited, carbonatisation is accurately quantified by normative methods. The normative estimate of CO<sub>2</sub> is helpful in exploration contexts, as CO<sub>2</sub> analyses carry extra analytical costs. In addition, the CONSONORM\_LG method distinguishes the phyllosilicates related to carbonatisation from those related to sericitisation and chloritisation [51].



As most alteration types are named after minerals, another advantage of normative calculations is to relate chemical analyses to petrological observations.

**Table 4.** Characteristics of normative methods.

Method—Normative Calculations and Related Indices	
<b>Advantages</b>	Accurate estimate of carbonatisation and other alterations Relatively independent of the composition of precursors
<b>Disadvantage</b>	Silicification, albitisation, and K-feldspar alterations are hard to quantify because marker alteration minerals are abundant in unaltered rocks
<b>Requirements</b>	Whole-rock chemical analyses (major elements) and basic knowledge of metamorphic assemblages (to select the proper P-T model)
<b>Recommendation</b>	Can be used in a variety of contexts Recommended if carbonatisation needs to be quantified

The CONSONORM\_LG method has been applied to 261 anorthosite and gabbro samples from the Chibougamau data set. This method is calculated for the 2SV350 model. The  $\text{Fe}_2\text{O}_3/\text{Fe}_2\text{O}_3^{\text{T}}$  ratio is about 0.2 for the 24 samples having FeO and  $\text{Fe}_2\text{O}_3$  analysed, and a ratio of 0.2 is used to estimate the iron values for the remaining samples.

For the Central Camp data,  $\text{CO}_2$  has been analysed for 92 samples, and these values correlate well with the normative  $\text{CO}_2$  values ( $r = 0.79$ ). The CONSONORM\_LG indices indicate that chloritisation, sericitisation, and phyllic alterations are moderate to intense for some samples (ALT\_CHLO, ALT\_MUSCV, ALT\_PARA, ALT\_PHYLLO) (Figure 2a). The other indices indicate that carbonatisation is moderate (ALT\_CARB), and that it did not produce white mica (ALT\_CARB > ALT\_MUSCV\_CARB). However, it may have formed some chlorite (for samples with ALT\_CARB < ALT\_CHLO\_CC\_TLC) (Figure 2a).

The CONSONORM\_HG method has been applied to the Arunta data set [39]. This method is calculated for the 9GRA800 model (meaning 800 °C and 9 kbar, which is close to the peak metamorphic conditions reported for the Arunta block [55]). The  $\text{Fe}_2\text{O}_3/\text{Fe}_2\text{O}_3^{\text{T}}$  ratio is about 0.2 for a portion of the samples, and a ratio of 0.2 was applied to estimate FeO and  $\text{Fe}_2\text{O}_3$  for the six remaining samples. Normative minerals can be displayed in a circle diagram (Figure 2b) similar to the one described by Mathieu et al. [14]. To plot a sample in a circle with radius R and centre with Cartesian coordinates (Cx, Cy), x and y coordinates are calculated using Equations (12) and (13), and using factors  $F_n$  and  $G_n$  to control the location of the displayed minerals ( $M_n$ ).

$$x = (M_1F_1 + M_2F_2 + \dots + M_nF_n)/(M_1 + M_2 + \dots + M_n - \text{quartz}) \quad (12)$$

$$y = (M_1G_1 + M_2G_2 + \dots + M_nG_n)/(M_1 + M_2 + \dots + M_n - \text{quartz}) \quad (13)$$

where:

- $M_1, M_2, \dots, M_n$ —proportions of the normative minerals displayed on the circle diagram;
- $F_1, F_2, \dots, F_n$ , and  $G_1, G_2, \dots, G_n$ —factors (e.g., to locate cordierite, the factors used are  $F_{\text{cord}} = Cx \cos(\pi/3) + R$  and  $G_{\text{cord}} = Cy \sin(\pi/3) + R$ ).

The circle diagram shows that, at Arunta, the chloritised rocks (i.e., cordierite quartzites) and their unaltered equivalents plot on different parts of the diagram; i.e., they have distinct normative mineral contents. As the altered rocks are enriched in garnet and cordierite (Figure 2b), an alteration index based on these minerals is used (Equation (14)) to conclude that chloritisation is moderate to intense (see box plots of Figure 2b).

$$\text{ALT\_CORD} = 100 \times (\text{cordierite} + \text{garnet})/(\text{sum of all silicates except quartz}) \quad (14)$$

The CONSONORM\_HG method has then been applied to 32 greywacke samples from the Roberto data set. This method is calculated for the 3AMP675 model (representing 675 °C and 3 kbar, which is close to the peak metamorphic conditions [42]). FeO and Fe<sub>2</sub>O<sub>3</sub> analyses are unavailable, and a Fe<sub>2</sub>O<sub>3</sub>/Fe<sub>2</sub>O<sub>3</sub><sup>T</sup> ratio of 0.2 is used because of the generally reduced nature of orogenic gold systems [56]. Normative minerals are displayed in a circle diagram (Figure 3), where the samples distribute between K- and Ca-bearing minerals in accordance with the documented K- and Ca-metasomatisms [40–42]. Alignment of some samples also suggests feldspar destruction and/or Fe-Mg-gains (Figure 3). However, without a clearly identified precursor, these alteration trends are speculative, and alteration indices are not calculated.

These examples illustrate the steps that need to be followed when using normative methods: (1) analyse major elements; (2) analyse or estimate FeO and Fe<sub>2</sub>O<sub>3</sub>; (3) estimate the P-T conditions of the metamorphic peak to select the appropriate normative model; (4) perform the calculation and analyse the results; and (5) use the default indices of the Normat and CONSONORM\_LG methods or select pertinent minerals (e.g., cordierite for chloritisation) to calculate the alteration indices. Normative calculations can be applied to rocks with sedimentary or igneous protoliths and they are particularly useful to exploration geologists working with historical data sets or to those who wish to estimate carbonatisation without incurring additional analytical costs.

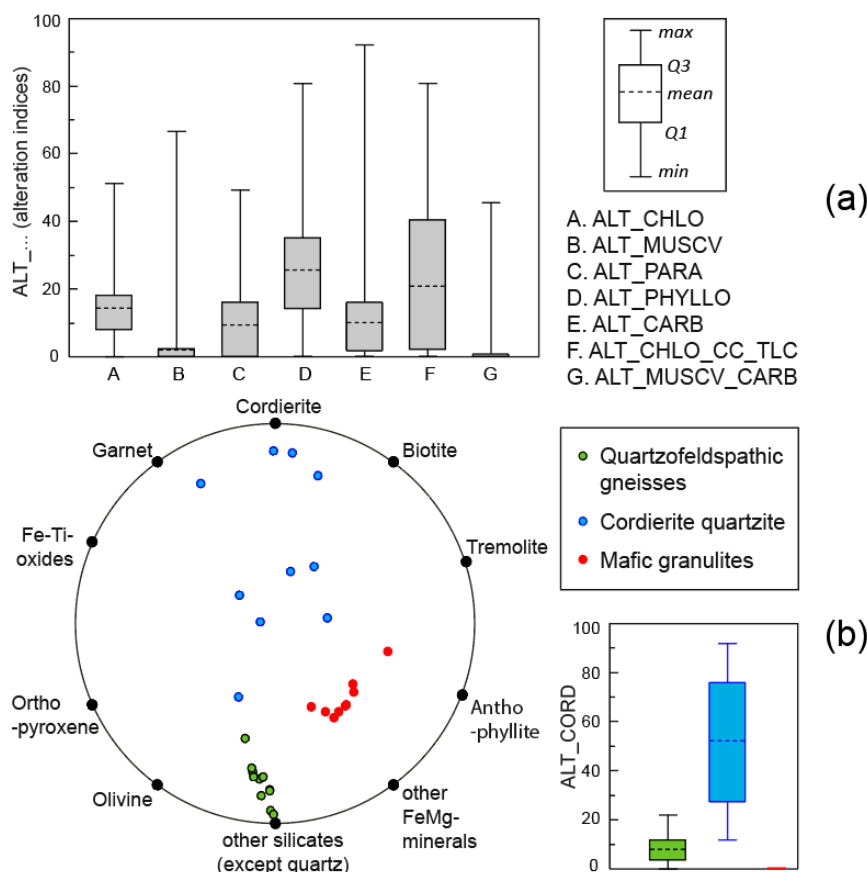


**Figure 2.** (a) Central Camp data set: indices of the CONSONORM\_LG method [51] displayed by box plots. These indices are designed to quantify: (1) chloritisation (ALT\_CHLO); (2) sericitisation (ALT\_MUSCV, ALT\_PARAG); (3) phyllic alteration (ALT\_PHYLLO); (4) carbonatisation (ALT\_CARB); (5) carbonatisation and white mica by-products (ALT\_MUSCV\_CARB); and (6) carbonatisation and Fe-Mg-minerals by-products (ALT\_CHLO\_CC\_TLC); (b) Arunta data set: normative minerals of the CONSONORM\_HG method [52] displayed on a circle diagram akin to the one described by Mathieu et al. [14], and ALT\_CORD index displayed by box plots.

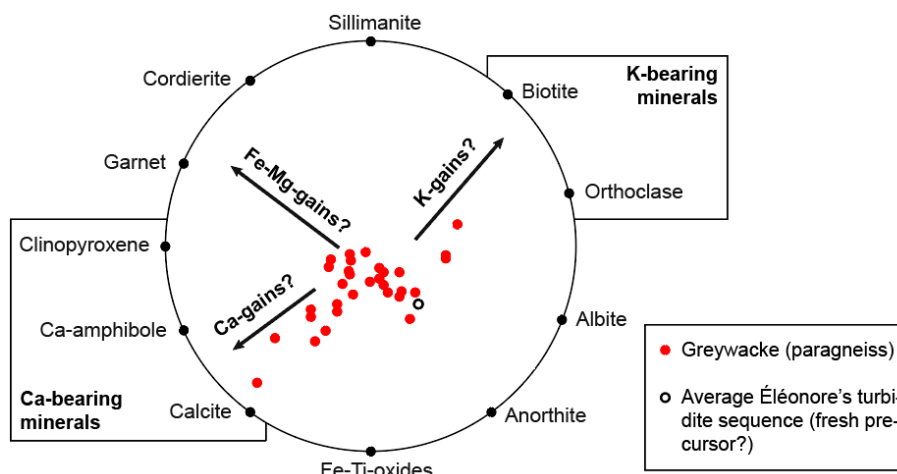


**Figure 3.** Normative minerals of the CONSONORM\_HG method [52] calculated with the Roberto data set and displayed on a circle diagram.

#### 4.3. Comparison of the Alteration Indices

Major element and normative mineral indices can be compared using the La Grande Sud data set; the selected alteration indices being calculated are the chlorite index [57], the sericite and albite saturation indices [16], and the K-feldspar saturation index (Figure 4). The carbonate saturation index [16] is also calculated when CO<sub>2</sub> analyses are available. The 2SV350 model of the CONSONORM\_LG method is run using analysed values of FeO and Fe<sub>2</sub>O<sub>3</sub>.

The Fe<sub>2</sub>O<sub>3</sub>/Fe<sub>2</sub>O<sub>3</sub><sup>T</sup> ratio is high (median = 0.65, standard deviation or std = 0.04), suggesting that the hydrothermal fluid was possibly oxidised. If these values had not been analysed, a modelled Fe<sub>2</sub>O<sub>3</sub>/Fe<sub>2</sub>O<sub>3</sub><sup>T</sup> ratio of 0.4 to 0.45—the mean ratio for sub-alkaline felsic igneous rocks [53]—would have been used, and this would have produced erroneous estimates of the proportions of Fe-Ti-oxides and Fe-Mg-silicates (e.g., chlorite). Normative pyrite can be determined as S analyses are available. The La Grande Sud samples contain <0.1 wt % normative sulphides (median = 0.07, std = 0.73).

The CO<sub>2</sub> normative estimates for the La Grande Sud data set correlate with the analysed values ( $r = 0.747$ ). Carbonatisation is moderate to intense (Figure 5a). Comparison between the ALT\_MUSCV\_CARB, ALT\_CHLO\_CC\_TLC, and ALT\_CARB indices suggest that carbonatisation induced the formation of little to no chlorite or white mica (Figure 5a).

Both the major element and normative mineral ratios point to intense carbonatisation (Figure 4e). Chloritisation, on the other hand, is moderate according to the chlorite index and negligible according to ALT\_CHLO (Figure 4a). As the normative method distributed iron between oxides, sulphides, and silicates, while the major element index considers only total iron, the normative results are likely more reliable.

The albite proportions correlate well with the albite saturation index (Figure 4c). The rocks contain a large amount of albite, and the indices show elevated values, which would be interpreted as albitisation if a least-altered sample (#19449) had not been identified. After comparison with this sample, feldspar destruction is inferred for most samples (Figure 4c). A similar remark can be made for K-feldspars. Normative K-feldspar is absent from Sample #19449, and the few samples that contain this mineral may have gained K (Figure 4d). The K-feldspar saturation index, on the other hand, suggests that most samples have gained K (in comparison with Sample #19449). The two methods are thus in disagreement and are probably both imprecise, given they consider only K-feldspar and white mica, while biotite is also reported in the tonalite [43]. In general, Na- and K-metasomatism are best quantified by mass balance methods (see next section).

Discrepancies are also observed for sericitisation, which either is overestimated by the sericite saturation index or is underestimated by ALT\_MUSCV (Figure 4b). As the normative calculation

distributes K between mica and feldspar, and as only mica is considered by ALT\_MUSCV, this index may be more reliable than the major element ratio.

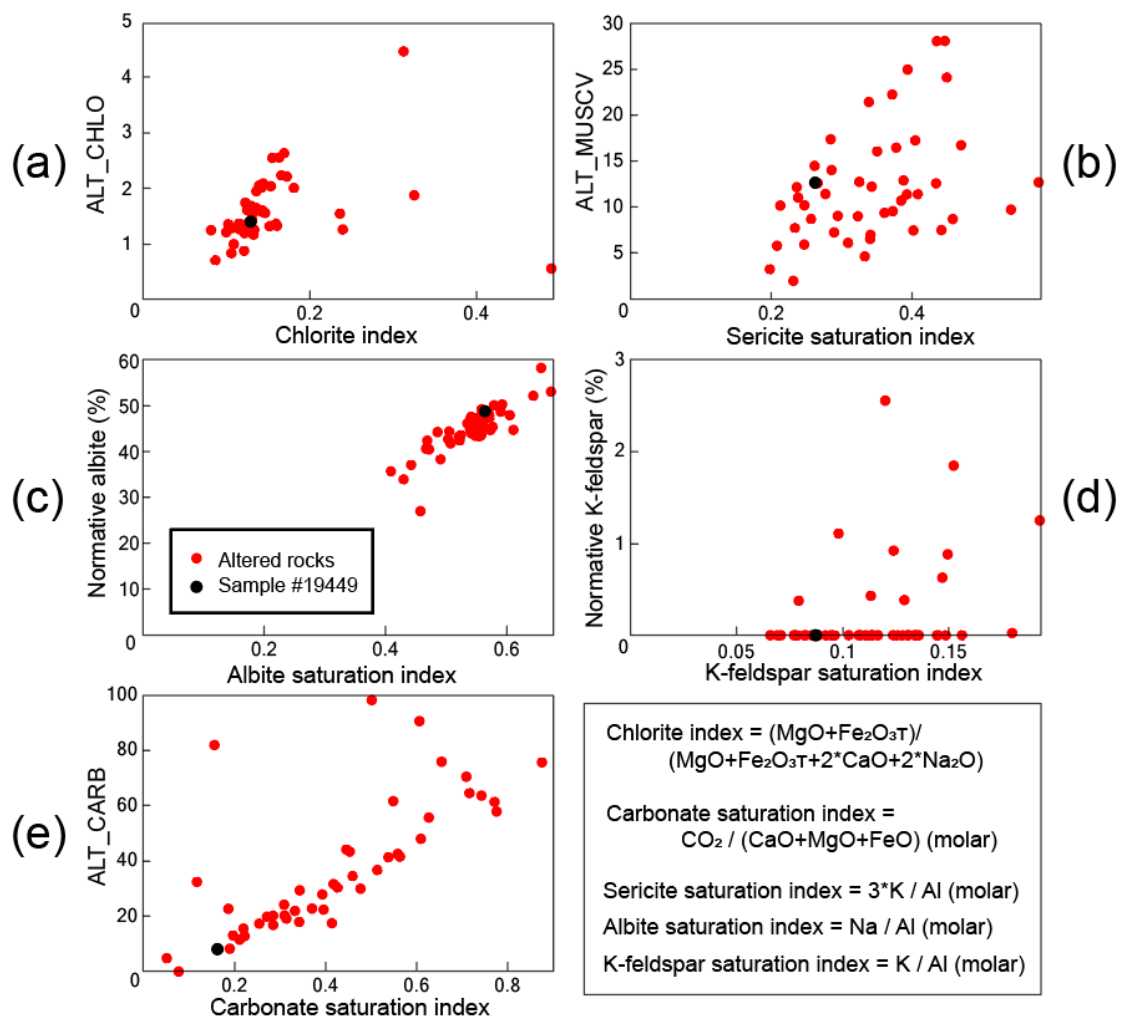


**Figure 4.** Binary diagrams comparing indices calculated using major elements (*x*-axis) and normative minerals (*y*-axis). These indices are designed to quantify (a) chloritisation, (b) sericitisation, (c) albitisation, (d) K-feldspar alteration, and (e) carbonatation.

To complete the comparison, the samples are displayed on the alteration box plot [26] (Figure 5b). The normative minerals are displayed on a similar diagram with axes defined (Equations (15) and (16)) to reflect the minerals displayed by the alteration box plot.

$$\text{Axis X} = 100 \cdot (\text{dolomite} \cdot 0.3 + \text{ankerite} \cdot 0.4 + \text{chlorite} + \text{pyrite} + \text{white mica} + \text{orthoclase}) / \text{sum} \quad (15)$$

$$\text{Axis Y} = 100 \cdot (\text{white mica} \cdot 0.25 + \text{epidote} + \text{calcite} + \text{dolomite} + \text{ankerite} + \text{chlorite} + \text{pyrite}) / \text{sum} \quad (16)$$

With sum = albite + epidote + calcite + dolomite + ankerite + chlorite + pyrite + white mica + orthoclase

On the original alteration box plot, the distribution of the samples suggests that the dominant processes are carbonatation and chloritisation (Figure 5b). On the modified diagram that uses normative minerals, the main alterations could be interpreted as K-metasomatism (sericitisation and/or K-feldspar alteration) and, for some samples, carbonatation. These observations are in agreement with the alterations reported by Mercier-Langevin [43], indicating that K-metasomatism is

best estimated by normative minerals rather than by major element ratios. In addition, carbonatisation appears moderate as the alteration box plot displays non-normalised carbonate proportions (Figure 5b). The intensity of carbonatisation is best quantified by dedicated indices (Figures 4e and 5a) that normalise carbonate proportions using Ca, Fe, and Mg.

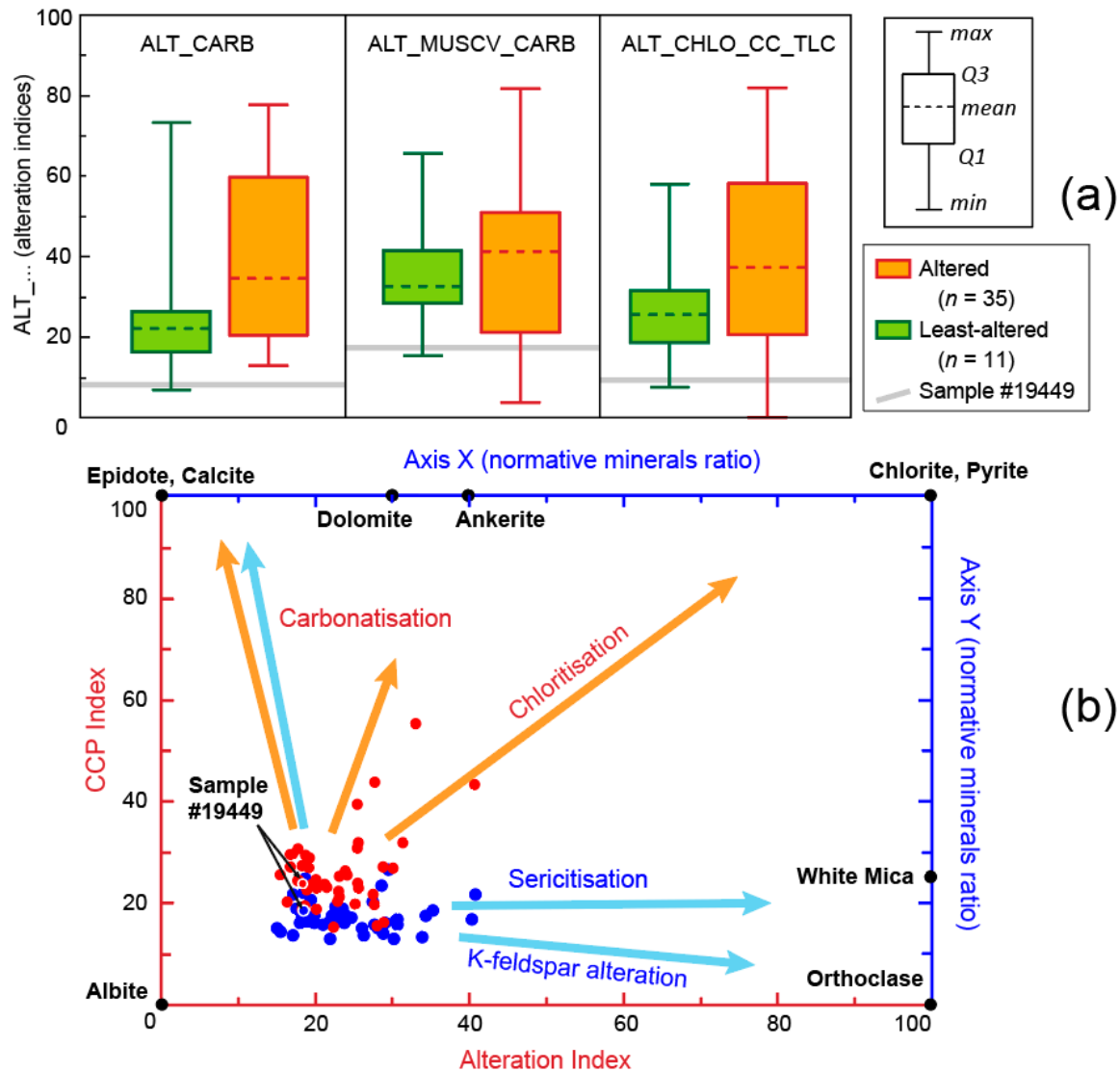


**Figure 5.** Results of calculations conducted on the La Grande Sud data set. (a) Indices of the CONSONORM\_LG method displayed by box plots. These indices are designed to quantify: (1) carbonatisation (ALT\_CARB), (2) carbonatisation and white mica by-products (ALT\_MUSCV\_CARB), and (3) carbonatisation and Fe-Mg-mineral by-products (ALT\_CHLO\_CC\_TLC); (b) Alteration box plot diagram [26] (in red) and an equivalent diagram (in blue) designed to display normative minerals.

## 5. Mass Balance Methods

The main difference between alteration indices and mass balance methods is that, while indices take mineralogical constraints into account, mass balance aims to quantify chemical changes. As field observations rely on alteration minerals, they are not always easily related to mass balance results. However, mass balance provides precise quantification of the amount of Si, Fe, Mg, K, Na, and Ca leached from the rock or brought in by the fluid. Another difference between the indices and mass balance methods is that the latter requires the analyses of some immobile trace elements and the identification of a precursor.

### 5.1. Mass Transfer Equation

Mass balance methods are based on the Gresens mass transfer equation [58,59]. These methods estimate volume and density changes (i.e., mass changes) induced by alteration. Density variations can be taken into account [60], but are generally neglected. Volume changes are estimated by comparing the content in immobile elements of the altered rock to that of its precursor. It is assumed that the absolute amount of these elements has not been modified by the alteration process [24]. Once the total volume (~mass) change is estimated, then the gain/loss of individual mobile elements is calculated by applying the mass transfer equation (Equation (17)) [24,58].

$$X_n = W_n^B - W_n^A = w \{[(F_V)(X_n^B)(S^B/S^A)] - X_n^A\} \quad (17)$$

where:

- $X_n$ —mass change of component n expressed in g per 100 g of precursor;
- $W_n^B - W_n^A$ —weight of component n in the precursor (A) and in the altered rock (B);
- $w$ —weight of precursor (=100 g usually);
- $X_n^A, X_n^B$ —component n in rocks A and B;
- $S^B, S^A$ —density of rocks A and B (often neglected);
- $F_V$  (volume ratio) =  $\text{volume}^A / \text{volume}^B = (\text{mass}^B / \text{mass}^A) * (S^A / S^B) \sim (\text{mass}^B / \text{mass}^A)$ .

If density is neglected, using Equation (17) requires the chemical compositions of the altered rocks and their precursors ( $X_n^A$  and  $X_n^B$ ), which are obtained from chemical analyses and/or modelling (see next section). The  $F_V$  factor is calculated using the  $\log(F_V)$  vs.  $\log(X_n)$  diagram (see Leitch and Lentz [24] for details), or using the slope of the isocon line (see below). The  $F_V$  factor can also be replaced by  $(X_{\text{immobile}}^A / X_{\text{immobile}}^B)(S^B / S^A)$ , which simplifies Equation (17) to Equation (18) [24,25].

$$X_n = w \{[(X_n^B) (X_{\text{immobile}}^A / X_{\text{immobile}}^B)] - X_n^A\} \quad (18)$$

The available mass balance methods use Equations (17) or (18) and various strategies to estimate total mass changes and precursor compositions. Three of these methods are presented in Section 5.3.

### 5.2. Errors, Precursors, and Immobile Elements

Quantifying alteration with mass balance methods requires analysed immobile elements as well as constraints on the chemistry of the precursor. Most errors associated with mass balance calculations are due to: (1) sampling and analytical errors; (2) erroneous precursor selection; and (3) the mobility of elements normally considered immobile. Analytical errors are easily avoidable with modern procedures and good practices [61], although performing representative sampling is more challenging [30,31] (Section 2.2).

Obtaining the composition of a precursor is difficult as, by definition, it corresponds to a rock that no longer exists. Fresh to least-altered equivalents of the altered rocks can, however, be found at a distance from the mineralised area and be used as precursors.

To select a precursor, it must be determined whether the system is chemically homogeneous or heterogeneous; i.e., does it have one or several precursors. Heterogeneities are due to, for example, fractional crystallisation or gravity sorting in igneous and sedimentary environments, or phenocrysts (a sampling issue). These heterogeneities can be visualised with immobile vs. immobile element diagrams that are used to relate a group of altered rocks to their most representative precursor, that is the freshest rocks that could be found in the field [18]. Alternatively, individual precursors can be modelled for each altered rock [62] (see next section).

In addition to selecting a precursor, mass balance calculations require the identification and analysis of immobile elements. By definition, an immobile element is neither added nor removed from the rock by the hydrothermal fluid. Commonly used elements include Ti, Al, Zr, Y, Nb, Th, Cr, Co,

and REE (rare earth elements) [45,62,63]. The immobility of these elements must be verified prior to performing any mass balance calculations. For example, LREE (light-REE) and Y are reported to be mobile in some VMS systems [45,64], and immobility is not guaranteed in the most extreme conditions, such as rocks in contact with F-bearing fluids [65].

In single precursor systems, Nb can be used to verify the immobility of an element (e.g., Al), as Nb is mobile only under the most extreme conditions. The verification is performed by ensuring that the Al/Nb ratio varies within a reasonable range [24,45]. In multiple precursor systems, variance analyses or binary diagrams are used to ensure that samples having similar precursors also have relatively constant immobile/immobile ratios. On the  $\text{Al}_2\text{O}_3$  vs.  $\text{TiO}_2$  diagram, for example, if the tested elements are immobile, then samples having similar precursors align along lines passing through the origin, and the correlation factor is  $>0.85$  [25]. Also, on such immobile-immobile diagrams and for co-magmatic units, fresh samples define a fractionation trend that can help in the selection of precursors [18].

### 5.3. Three Mass Balance Methods

The isocon, immobile element, and modelled precursor methods are three complementary mass balance methods that calculate mass changes with different strategies, using a few to many immobile elements as well as sampled or modelled precursors.

The isocon method [66,67] is similar to the straight-line diagram [68] and other solutions [69–71]. This graphical method compares an altered sample to its precursor (Figure 6) to estimate the volume change (Fv factor) necessary to the calculation of mass changes with Equation (17). On a binary diagram, the immobile elements align along the isocon line, which passes through the origin, and the total volume change equals the inverse of the slope of this line (Figure 6a). Poor alignments of immobile elements are generally due to non-representative precursors. This method estimates mass changes from several immobile elements and provides accurate results for single precursor systems; for example, a lava flow unit having a documented limited chemical heterogeneity. However, this approach can be tedious as it requires that a diagram be produced for each sample (Table 5).

The immobile element method uses a simplified Gresens equation (Equation (18)); it can be applied easily and rapidly to large data sets. This method was proposed in the 1980s [72] and fully developed in the 1990s [25,73–76]. It has the advantage of acknowledging the chemical heterogeneity of natural rocks, that is it facilitates the processing of multi-precursor systems (Table 5). Chemical variations of related rocks (e.g., co-magmatic igneous rocks) are displayed on immobile vs. immobile element binary diagrams (Figure 6b), which are used to segment the data sets into groups of rocks having similar precursors. Least-altered samples are then selected within each group to serve as precursors, and Equation (18) is then applied [18]. The immobile element used to calculate Equation (18) can be Zr, Nb, or else, as long as immobile elements are well correlated ( $r > 0.85$ ) [25] within groups of rocks having similar precursors.

Both the immobile elements and the isocon methods require the sampling of a fresh or least-altered rock as representative as possible of the precursor. Most of the imprecision in mass balance calculations is due to inappropriate precursor selection, either because a given unit is entirely altered (e.g., a small-volume intrusion), because the sampling is not representative (e.g., phenocryst-enriched rocks), or because natural systems are more chemically heterogeneous than assumed. An alternative method has been proposed that uses the immobile element content of a rock to model the composition of its precursor [62]. Each sample can thus be compared to a “personalised” precursor. The modelled precursor method applies to rocks having a predictable chemistry, such as igneous rocks, and is ideal for poorly documented areas where the sampling of a fresh precursor is challenging (Table 5). Once the precursors are predicted, any variant of the mass transfer equation can be applied.

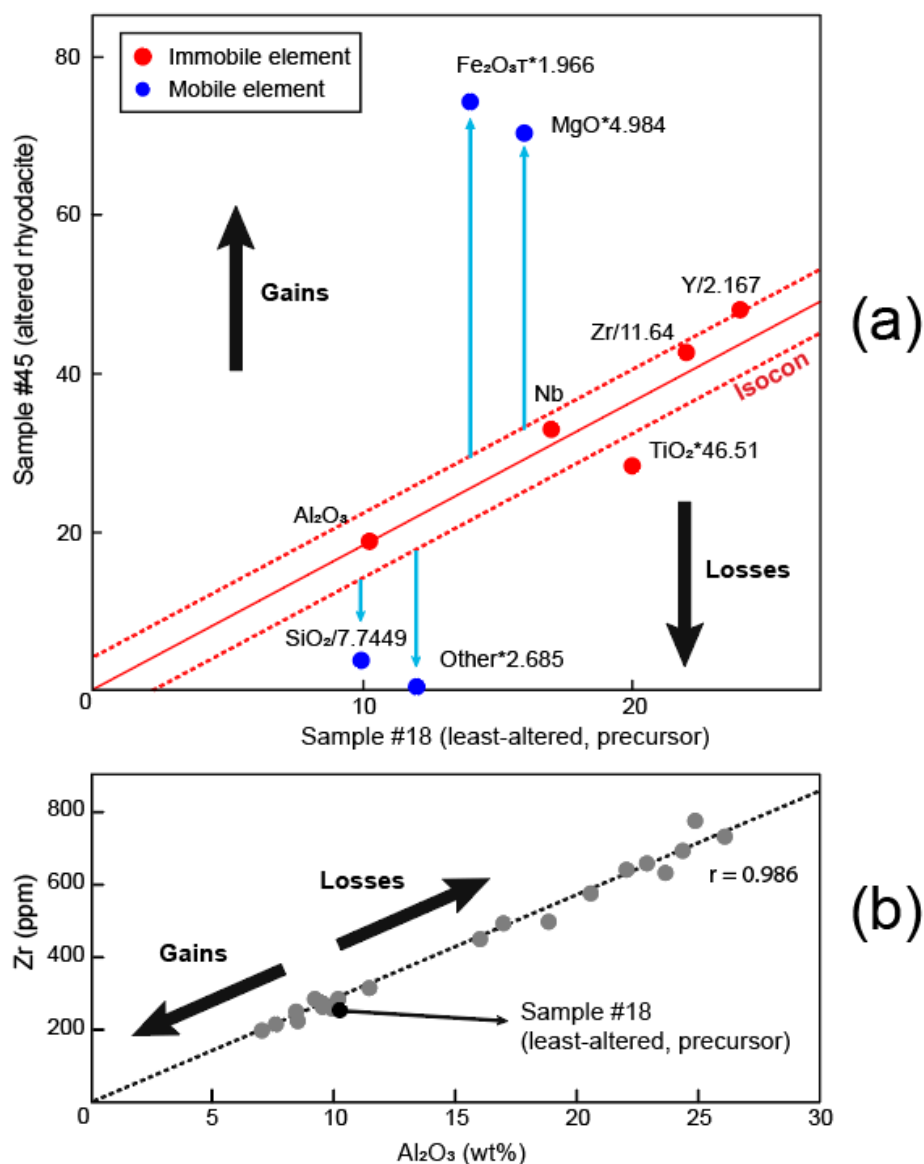


**Figure 6.** (a) Example of an isocon diagram that compares rhyodacite samples #18 and #45 (Phelps–Dodge VMS), which are described as least-altered and altered, respectively [45]. The “other” elements correspond to  $\text{Na}_2\text{O} + \text{K}_2\text{O} + \text{CaO}$ . The elements are multiplied by factors depicted on the diagram (for a discussion of these factors, refer to Baumgartner and Olsen [77]); (b) Immobile-immobile diagram displaying rhyodacite samples (single precursor system) of the Phelps–Dodge deposit [45].

#### 5.4. Interpretation of the Results

Global mass changes, i.e., the amount of mass transferred into or out of a rock by a fluid, are approximated by volume changes. They are used to locate, for example in shallow systems, the area that developed a porosity (global mass loss) and that was favourable for fluid circulation and ore deposition. More accurate volume changes can also be calculated if density data are available. Despite its importance for various aspects of a mining project, such as estimating tonnage, density is not always measured. It can alternatively be estimated from normative calculations [78].



**Table 5.** Characteristics of mass balance calculations.

<b>Mass Balance Calculations—Generalities</b>	
<b>Advantage</b>	Quantify mass gains and losses for each mobile element
<b>Disadvantage</b>	Chemical method that can be hard to reconcile with mineralogical observations, as alteration types bear the name of minerals, not chemical elements
<b>Requirements</b>	Whole-rock chemical analyses (at least major and minor elements); analysed and identified immobile elements
<b>Method #1—Isocon Analysis</b>	
<b>Advantage</b>	Precise mass balance calculation that can be used on all rock types
<b>Disadvantages</b>	Requires the sampling of a fresh rock that closely resembles the precursor of the studied altered rock Tedious in its application Only for rocks having similar precursors (single precursor systems)
<b>Recommendation</b>	To be used in well-documented areas
<b>Method #2—Immobile Elements</b>	
<b>Advantages</b>	Precise mass balance calculation for multiple precursor systems Simple to use
<b>Disadvantages</b>	Requires the sampling of a fresh rock that closely resembles the precursors of each rock type Mostly applied to co-magmatic igneous rocks, but it could be adapted to sedimentary rocks
<b>Recommendation</b>	To be used in well- to relatively well-documented areas
<b>Method #3—Modelled Precursors</b>	
<b>Advantages</b>	Designed for grassroots exploration (i.e., poorly documented areas) Does not require precise constraints on the composition of precursors
<b>Disadvantages</b>	Applies only to igneous rocks Complex, but software solutions are available [62]
<b>Recommendation</b>	Use in poorly to well-documented areas, as long as the precursor is an igneous rock and Zr is analysed

Results of mass balance calculations are generally interpreted for individual elements. The results of mass balance calculations are presented: (1) in percentage, which corresponds to mass changes relative to the composition of the precursor; and (2) in grams per 100 g of precursor, which corresponds to absolute mass changes. Leaching can thus be assessed through a relative mass change (did the rock lose all the mass that it could have lost?) or absolute (how much mass was lost?). In some cases, leaching is best expressed with relative values, as losses expressed in grams can be biased by the composition of the precursor—a mafic rock has more Ca and Mg to lose than a felsic rock.

Mass gains, on the other hand, are best documented using absolute results, as the amount of a mobile element gained (i.e., brought by the fluid) is independent of the composition of the precursor, as an example, Si-gains being related to the formation of quartz veins (infilling). In other cases, mass gains may be dependent of the composition of the precursor, and absolute mass gains must be interpreted with care. For example, the maximum amount of CO<sub>2</sub> that can be gained may depend on the Fe, Mg, and Ca content of the rock, and the maximum amount of K-gain, which produces alteration minerals such as feldspar or mica, is dependent on the Al-content of a rock. Relating mass changes to the intensity of the alteration process is thus not always straightforward, even when using mass balance calculations.

The error associated with mass balance methods is rarely assessed [79]. Insights into the imprecision of these methods are however necessary to interpret the results. Applying the modelled precursor method to fresh volcanic rocks (Table 2), mass changes <1 g (or >−1 g) per 100 g of precursor are obtained for most elements, except SiO<sub>2</sub> (±10 g per 100 g of precursor). These values likely fall within the imprecision of the method and correspond to negligible alteration. With the isocon and immobile elements methods, most of the error is likely associated with precursor selection and negligible alteration may correspond to different values, depending on the context.

### 5.5. Natural Examples

Mass balance calculations can be run for the 22 samples of the Phelps–Dodge data set [45]. The elements identified as immobile are Zr, Y, Nb, Ti, and Al [45]. The isocon method is applied using these five immobile elements, and the least-altered rock identified by MacLean and Kranidiotis [45] (Sample #18) is used as a precursor. The immobile element method is applied using the same precursor and Zr, while modelled precursors are calculated using Al, Zr, Ti, and Y as immobile elements. The three methods reproduce the documented chloritisation and Si-gains and losses [45] (Figure 7). The intensity of the alteration process, as estimated by the isocon and immobile element methods, is similar. The modelled precursor method, however, indicates that the sampled precursor is an altered rock, and that the intensity of chloritisation and silicification is underestimated by the other two methods (Figure 7). The modelled precursor method also indicates that chloritisation is intense—Fe + Mg gain up to 35 g per 100 g of precursor.

Mass balance calculations are also performed on the 47 samples of the La Grande Sud tonalite [43]. The isocon and immobile elements methods are applied following the procedure applied by Mercier-Langevin [43], using Sample #19449 as a precursor. Among the trace elements analysed, several are close to the detection limit (e.g., Cr, Nb, Th), and only Zr, Al, and Ti can be used to perform the isocon and modelled precursor calculations. Only Zr is used for the immobile element method. The  $\text{Al}_2\text{O}_3/\text{Zr}$ ,  $\text{TiO}_2/\text{Zr}$ , and  $\text{TiO}_2/\text{Al}_2\text{O}_3$  ratios have median (M) and standard deviation (std) values of 0.234 (M)-0.023 (std), 0.0024 (M)-0.0002 (std), and 0.0099 (M)-0.0007 (std), respectively. These ratios vary within a reasonable range, and the intrusion is considered to be a single precursor system.

The three methods indicate that Fe, Mg, and Si mass changes are limited to negligible (Figure 8a). The Si-gains likely correspond to quartz veins bearing samples, while the Fe- and Mg-gains may correspond to pyrite-bearing samples or to limited chloritisation. The isocon and immobile element methods also point to K-gains, and the result is in agreement with the reported K-metasomatism [43] (Figure 8b). These methods also indicate some Na-gains (immobile element method) and losses (both methods), which are in agreement with the reported feldspar destruction, i.e., sericitisation [43]. The reported inverse correlation between Na and K mass changes [43] is also observed for some samples and likely corresponds to alkali exchanges within the feldspars.

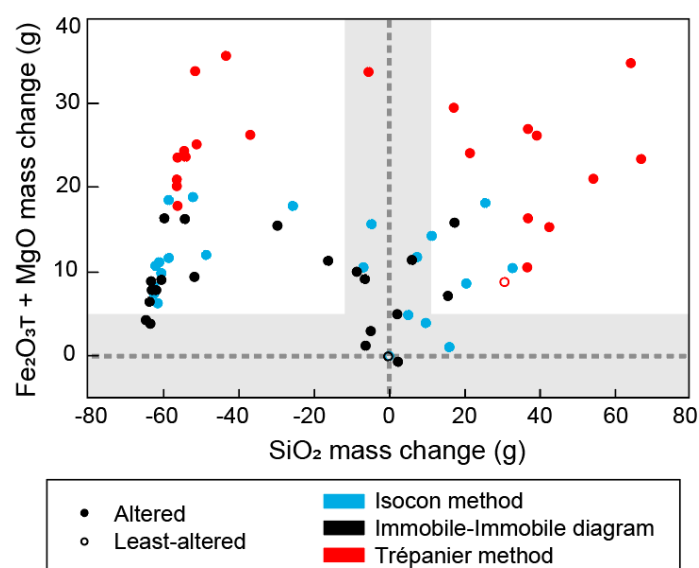


**Figure 7.** Fe + Mg vs. Si absolute mass change diagram of the mass balance calculations performed on 22 samples [45] from the Phelps–Dodge VMS. The grey area corresponds to negligible mass changes likely following within the error associated with each method.

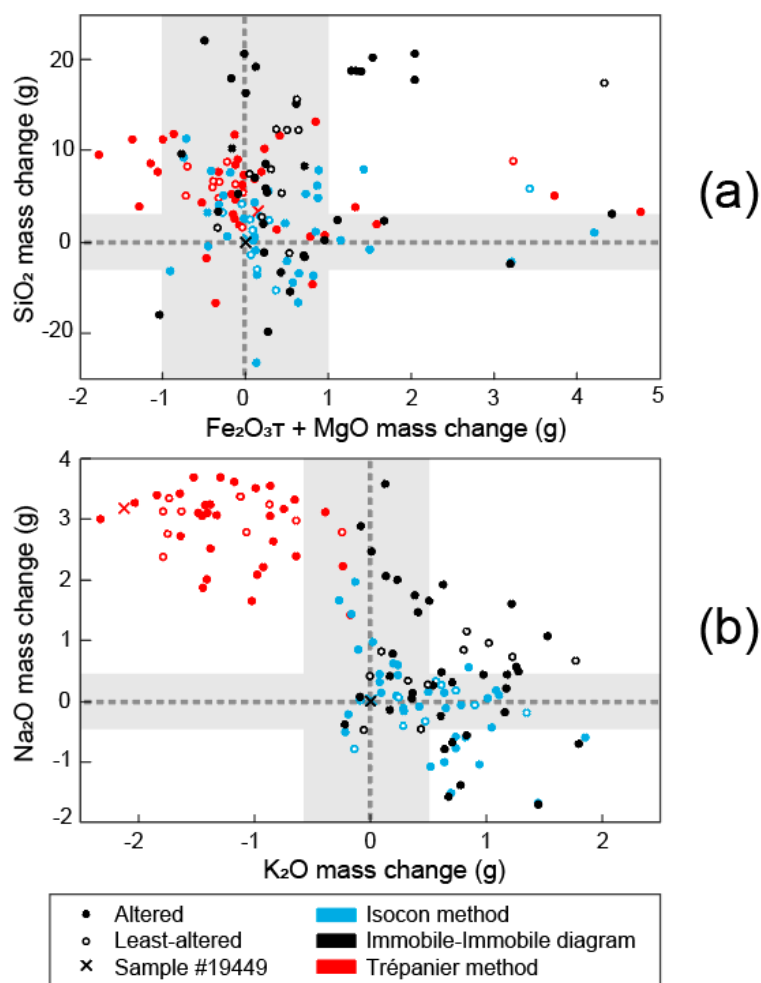


**Figure 8.** Binary diagram of the mass balance calculations run on 47 samples [43] from the La Grande Sud intrusion: (a) SiO<sub>2</sub> vs. FeO + MgO; and (b) Na<sub>2</sub>O vs. K<sub>2</sub>O absolute mass change. The grey area corresponds to negligible mass changes likely following within the error associated with each method.

The modelled precursor method, on the other hand, points to K-losses and Na-gains (Figure 8b), a result in disagreement with field and petrological observations [43]. A likely explanation is that the K-content of the modelled precursors has been overestimated. Indeed, rocks of the tonalite-trondhjemite-granodiorite (TTG) series are characterised by elevated Na/K ratios. However, these rocks are restricted to the Archean period, while the data set used to calibrate the modelled precursor method mostly contains samples from post-Archean igneous rocks [62]. This method is not suitable for rock types poorly represented in the data set used to train the neural network (e.g., komatiite, TTG, sanukitoid, lamprophyre, cumulate, pegmatite-bearing samples) [62]. However, considering Sample #19449 as least-altered, the modelled precursor method indicates that the tonalite has mostly gained K and has lost some Na (Figure 8b). This agrees with the results obtained via the other two methods.

## 6. Discussion

The intensity of a hydrothermal process can be estimated using distinct strategies; by taking mineralogical constrains into account (alteration indices) or by focusing on chemical changes (mass balance calculations). These complementary approaches can provide greater insight into alteration processes. When working with incomplete data sets, at least one of the available methods can usually be applied (Table 6).

### 6.1. Requirements for the Presented Methods

In an exploration context, a large amount of whole-rock chemical analyses can be performed on surface and underground samples. The most popular methods for the quantification of alteration are these that can make use of this wealth of analyses. For this reason, alteration indices—calculated using major elements or normative minerals—and mass balance calculations are the main methods favoured in exploration work to identify and target mineralisation using altered rocks. These methods are generally sufficient to document the alteration style and to locate the most intensely altered zones.

Most of the data sets used in this contribution are incomplete, and they illustrate a wide range of situations to which an exploration geologist may be confronted. Most data sets are generally suitable for the calculation of alteration indices, except those for which major element analyses are incomplete (e.g., the Phelps–Dodge data set) (point F on Table 6) or absent (e.g., “assay” analyses that document metal concentrations only).

In addition, alteration indices calculated using normative minerals can be imprecise if FeO and Fe<sub>2</sub>O<sub>3</sub> analyses are unavailable (e.g., the Phelps–Dodge data set). Indeed, one of the main advantages of a normative calculation is its ability to distribute iron between oxides, carbonates, and silicates. Normative methods can thus provide precise estimates of the amount of, for example, chlorite, as long as the values of FeO and Fe<sub>2</sub>O<sub>3</sub> are available (point A on Table 6). Because these analyses carry an extra cost, it is recommended to analyse FeO and Fe<sub>2</sub>O<sub>3</sub> for some samples (~5–10 samples per lithological unit) and to then use these analyses to estimate the Fe<sub>2</sub>O<sub>3</sub>/Fe<sub>2</sub>O<sub>3</sub><sup>T</sup> ratios of the remaining samples. In addition, if the samples contain >0.5–1 vol% sulphides, normative methods require S analyses to discriminate the Fe of the sulphides from that contained in the other minerals (see [52] for discussion). It is recommended to suppress mineralised samples from data sets lacking S analyses, prior to performing normative calculations.

Mass balance calculations (isocon and immobile element methods) can only be performed if some immobile elements are analysed (point B on Table 6) and if a precursor is available. The calculations performed on the compiled data sets are generally imprecise because the selected precursor is least-altered, not fresh (point C on Table 6). The modelled precursor method solves the problems associated with the sampling of a precursor but additional restrictions apply, as the method can only be applied if Zr, at the least (point B on Table 6), is analysed and if the precursor is an igneous rock well represented in the data set used to train the neural network (point D on Table 6) [62]. The Na-enriched rocks of the La Grande Sud data set, for example, are not suitable for this method.

Additional restrictions apply depending on the composition of the precursor. Indeed, alteration is generally quantified for rocks having igneous precursors, which are, for example, the most frequent hosting materials of VMS and porphyry. However, the hosting materials may also be sedimentary (e.g., the Roberto data set). In such contexts, to use alteration indices or the isocon method, a precursor must be sampled and demonstrated to be chemically homogeneous (Table 7). The major and trace element contents of sedimentary rocks may vary independently; as such, extending the modelled precursor method to sedimentary rocks is challenging [62]. For the same reason, the immobile method has been designed for igneous rocks only [18]. However, if it can be demonstrated that rocks having similar trace element ratios also have precursors with a similar major element content, then this method should be applicable in sedimentary contexts.

The described methods can be applied, however, on any metamorphic rock, as long as metamorphism-induced chemical changes are negligible compared to those caused through hydrothermal processes. At Arunta, migmatization may have induced significant chemical changes and the presented results may be imprecise (point E on Table 6). In some deposits, such as the Challenger orogenic gold deposit, post-mineralisation high-grade metamorphism has induced extensive anataxis [80]. In such contexts, the methods described here may reflect melting-related variations and would likely miss any alteration-related modifications. Metamorphism also induces de-volatilisation that makes it challenging to identify carbonatisation, for example. Apart from these

restrictions, alteration is quantified similarly whether or not the rocks were metamorphosed after the mineralising event.

The La Grande data set is suitable for all the presented methods. Carbonatisation, in this context, is interpreted using alteration indices, which also suggest K-metasomatism. However, K-gains are best quantified by mass balance calculations. The methods presented in this contribution are thus complementary and, whenever possible, it is recommended to compare indices and mass changes to identify and quantify alteration.

## 6.2. A Method for each Alteration Process

The methods presented in this contribution should provide insights into any alteration process. However, some methods are more suitable than others for quantification of specific alteration types.

Carbonatisation, for example, can only be estimated by some of the methods (Table 7). In addition, major element ratios and mass balance methods require CO<sub>2</sub> analyses, which are not always performed in an exploration context. Indeed, the most effective alteration indices are those that normalise the amount of CO<sub>2</sub> by Fe, Mg, and Ca (see the La Grande Sud example; Figure 4e), while indices that use only Ca, Fe, and Mg (e.g., CCPI) produce a poor estimate of the intensity of this process (Figure 5b). Carbonatisation is best quantified by normative methods capable of estimating CO<sub>2</sub> [17,51]. These methods have the additional advantage of distinguishing chlorite and white mica formed as a result of the carbonatisation process from those formed by sericitisation and chloritisation processes (e.g., Central Camp data set; Figure 2a).

Chloritisation is a form of alteration that is generally easy to quantify, due to the extent of the chemical modifications that it induces in a rock (i.e., feldspar destruction and Fe–Mg-gains), and it can be accurately estimated by any of the methods presented here (Table 7). Chloritisation is particularly intense and easy to quantify in VMS systems (e.g., the Hongtoushan and Arunta data sets). Similar remarks can be made for sericitisation. The advantage of mass balance methods over alteration indices is their ability to discriminate Fe- from Mg-metasomatism; this is important as Fe-enriched rocks can be the most proximal to mineralisation [27]. In addition, mass balance can indicate whether or not the formation of white mica is accompanied by K-gains (Table 7).

**Table 6.** Methods that can be applied to the selected data sets to quantify the intensity of alteration processes.

Data Set	Reported Alteration	Major Element Ratios	Normative Methods	Isocon Method	Immobile Element Method	Modelled Precursors
Hongtoushan	Chl <sup>1</sup>	Yes	Imprecise (A <sup>2</sup> )		Imprecise (B, C)	No (B)
Chibougamau	Si, Carb, Chl, Ser	Imprecise (C)	Yes		Imprecise (B, C)	Imprecise (D)
Arunta	Chl	Imprecise (E)	Imprecise (E)		Imprecise (B, E)	No (B)
Roberto	Calc, Si, K	Imprecise (C)	Imprecise (A, C)		Imprecise (B, C, D)	No (B, D)
La Grande Sud	Si, Carb, K, Ser, Prop	Yes	Yes	Yes	Yes	Imprecise (D)
Phelps–Dodge	Chl, Si	No (F)	No (A, F)		Yes, for some major elements (F)	

<sup>1</sup> Abbreviations used: Si (Silicification), Carb (carbonatisation), Chl (chloritisation), Ser (sericitisation), Calc (calc-silicate veins), K (K-feldspar alteration), Prop (propylitic alteration). <sup>2</sup> A—no FeO and Fe<sub>2</sub>O<sub>3</sub> data included (only Fe<sub>2</sub>O<sub>3</sub><sup>T</sup> being available for most samples); B—trace elements are lacking for most samples; C—lack of petrographic observations (i.e., no precursors identified) or only altered rocks available (i.e., no fresh rock that can be used as a precursor); D—igneous precursor that is poorly represented in the data set that was used to train the neural network, or precursor that is not an igneous or meta-igneous rock; E—migmatite reported, meaning that metamorphism may have produced important chemical modifications; F—incomplete major element analysis.

Silicification, K-feldspar alteration, and albitisation form alteration minerals (quartz and feldspar) that are abundant in fresh rocks. As such, alteration indices can be hard to interpret if the composition of the precursor is unavailable. For example, the alteration indices calculated with the La Grande Sud data set indicate albite destruction and poorly estimate K-metasomatism (Figure 4), while mass balance calculations point to moderate Na-losses and K-gains.

For such alteration types, mass balance calculations are generally more reliable (Table 7). The La Grande Sud example shows, however, that alkali metasomatism is one of the most difficult alteration types to quantify (for another example, see [15]). Indeed, alkali elements are particularly mobile. As a result, it is not always possible to estimate their concentration in the precursor. This can lead to erroneous estimates when applying the isocon and immobile element methods. In addition, K and Na are not always modelled accurately [62].

Regardless of the selected method, trends can generally be interpreted in terms of increasing alteration intensity (e.g., Figure 8b). Interpreting absolute values is more challenging if the precursor is a least-altered rock (e.g., Figure 7). In the La Grande Sud example, K-gains of +1–2 g per 100 g of precursor point to moderate to intense K-metasomatism, in comparison with calculations performed on samples from porphyry systems (see Figure 10 of Trépanier et al. [62]). However, if the least-altered rock used as a precursor has undergone feldspar destruction or K-metasomatism, then these values will be underestimated or overestimated, respectively.

**Table 7.** Suitable methods for the quantification of alteration.

	Major Element Ratios	Normative Methods	Isocon Method	Immobile Element Methods	Modelled Precursor
Silicification, K-feldspar, albitisation	Hard to interpret if precursor is unavailable		Accurate quantification if precursor is representative		
Carbonatisation, propylitic alteration	If CO <sub>2</sub> analysed	Yes	If CO <sub>2</sub> analysed	No	
Sericitisation	K-gains or losses are hard to discriminate		Precise quantification of alkali gains/losses; can be hard to relate to white mica proportions		
Chloritisation	Yes	Yes, often better	Yes, and can distinguish Fe- from Mg-gains		
Sedimentary precursor	Only if a representative precursor is identified			No	No

### 6.3. Recommendations and Alternative Methods

All the methods used for the quantification of alteration intensity have both advantages and disadvantages (see summaries in Tables 3–5). In general, in well-mapped areas having documented precursors, most alteration processes can be quantified using alteration indices. In fact, in well-documented mono-precursor systems, even single elements can be used, such as Na to assess feldspar destruction [81] or trace elements to document the distal expression of alteration halos [2,82].

Normative methods are particularly useful if carbonatisation needs to be quantified without extra analytical costs. Furthermore, such methods are interesting because they link field observations with chemical analyses. Normative methods are also an alternative to mineral counts even if, ideally, the calculation should be validated using thin sections [14]. Indeed, petrological studies provide more accurate estimates of mineral proportions, reveal the texture of minerals and veins, and provide insights into cross-cutting relationships (for overlapping alterations). Where successive processes are postulated (e.g., Phelps-Dodge), petrographic observations could validate the interpretations made using binary diagrams (Figure 7).

The techniques described in this contribution consider whole-rock analyses. Hydrothermal systems can also be investigated with alternative technics, which rely on the chemistry of individual minerals used as tracers [83], while others focus on the nature of the fluid (using fluid inclusions [84]) or on its temperature (using stable isotopes—see for example [85,86]).

Regardless of the preferred approach, mass balance calculations remain the most reliable way to quantify the gain or loss of major elements by a rock. Once trace elements are analysed and their immobility tested, the most critical step is selecting a precursor. Sampling or modelling of precursors is only possible under certain circumstances (Tables 6 and 7) and must be performed with care. An alternative method is the Pearce element ratio diagrams [87] applied to altered rocks [12]. This approach uses the natural chemical heterogeneity of rocks to test hypotheses and requires neither

sampled nor modelled precursors. However, it only applies to well-documented magmatic contexts and is only useful under certain circumstances [15]. In poorly documented areas, it is recommended to remove sedimentary rocks and unusual igneous rocks (e.g., ultra-K rocks) and to apply the modelled precursor techniques. In well-documented areas, however, it is best to sample representative precursors and to apply the immobile element method that is more practical than the isocon method.

## 7. Conclusions

Alteration indices and mass balance calculations are popular methods among exploration geologists; they can be applied to the wealth of whole-rock chemical analyses generated by a mining project, and they are generally sufficient to document the extent and intensity of alteration processes. The methods presented in this contribution quantify alteration through various strategies and provide complementary insights into the alteration process. Whenever possible, it is recommended to apply several methods and to compare the results. In complex settings, where several alteration events overlap, these techniques can still be useful. However, they require careful interpretation. In such cases, it is best to use diagrams capable of displaying several alteration trends (e.g., Figure 7).

Several alteration indices and mass balance calculations methods were applied to 6 datasets to conclude that:

1. Major element ratios are alteration indices easy to calculate and best applied to well-documented areas;
2. Normative mineral ratios provide a reliable quantification of carbonatisation and can help relate observed metamorphic minerals to chemical data;
3. The isocon mass balance method is suitable for single precursor systems having well-documented precursors. It can be tedious in its application but has the advantage to rely on several immobile elements;
4. The immobile element method is a more practical mass balance method that is particularly effective in multi-precursor systems; and
5. The modelled precursor mass balance method solves the precursor sampling issue but can only be applied to common igneous rocks.

Future research should focus on evaluating uncertainty (e.g., [79]) and on the interpretation of alteration indices and mass balance results; for example, establishing more precise values for the terms “weak”, “moderate”, and “intense” alteration. Improved precision can be achieved by compiling data from a wide range of settings and then applying petrographic observations and various calculations. Exploration models will also benefit from a larger-scale approach (e.g., current Metal Earth project led by the Laurentian University, Sudbury, ON, Canada) that aims at understanding mineralising systems as a whole, rather than focusing on individual deposits. Finally, alternative methods could study alteration using whole-rock analyses. Machine learning techniques, such as genetic algorithms [88], could be used, for example, to document evolving hydrothermal systems and to develop methods that do not require the sampling of a precursor.

**Funding:** This research was funded by Canada First research Excellence Funds.

**Acknowledgments:** This manuscript was greatly improved by comments of two anonymous reviewers. This study was undertaken as part of the Metal Earth project (Laurentian University) investigation of the Chibougamau area, and this research was funded by Canada First research Excellence Funds. The author is indebted to the many collaborators of this project, including Harold Gibson, Bruno Lafrance, and Ross Sherlock. The author developed her ideas regarding hydrothermal alteration between 2012 and 2017 while she worked for the CONSOREM research group (Consortium de Recherche en Exploration Minérale). This research was thus also funded by Canada Economic Development for Québec Regions, the Ministère de l'Énergie et des Ressources Naturelles du Québec (MERN), the Conférence Régionale des Élus Saguenay-Lac-Saint-Jean (CRÉ), and the industrial members of CONSOREM. The author gives warm thanks to Sylvain Trépanier for the many discussions on hydrothermal alteration. Thanks are also given to the CONSOREM group, in particular Réal Daigneault, Silvain Rafini, and Stéphane Faure, and to the individual members of CONSOREM for many stimulating discussions over the years. This is Metal Earth contribution number MERC-ME-2018-024.

**Conflicts of Interest:** The authors declare no conflict of interest.

## References

1. Large, R.R.; McGoldrick, P.J. Lithogeochemical halos and geochemical vectors to stratiform sediment hosted Zn-Pb-Ag deposits, 1. Lady Loretta Deposit, Queensland. *J. Geochem. Explor.* **1998**, *63*, 37–56. [[CrossRef](#)]
2. Eilu, P.; Groves, D.I. Primary alteration and geochemical dispersion haloes of Archaean orogenic gold deposits in the Yilgarn Craton: The pre-weathering scenario. *Geochem. Explor. Environ. Anal.* **2001**, *1*, 183–200. [[CrossRef](#)]
3. Cooke, D.R.; Baker, M.; Hollings, P.; Sweet, G.; Chang, Z.; Danyushevsky, L.; Gilbert, S.; Zhou, T.; White, N.C.; Gemmill, J.B. New advances in detecting the distal geochemical footprints of porphyry systems-epidote mineral chemistry as a tool for vectoring and fertility assessments. In *Building Exploration Capability for the 21st Century*; Kelley, K.D., Golden, H.C., Eds.; Colt Print Services: Boulder, CO, USA, 2014; pp. 127–152, ISBN 978-1-629491-424.
4. Phillips, G.N.; Powell, R. Formation of gold deposits: A metamorphic devolatilization model. *J. Metamorph. Geol.* **2010**, *28*, 689–718. [[CrossRef](#)]
5. Morogan, V. Mass transfer and REE mobility during fenitization at Alno, Sweden. *Contrib. Mineral. Petrol.* **1989**, *103*, 25–34. [[CrossRef](#)]
6. Sillitoe, R.H. Porphyry copper systems. *Econ. Geol.* **2010**, *105*, 3–41. [[CrossRef](#)]
7. Robert, F. Syenite-associated disseminated gold deposits in the Abitibi greenstone belt, Canada. *Miner. Depos.* **2001**, *36*, 503–516. [[CrossRef](#)]
8. Stanton, R.L. Magmatic evolution and the ore type-lava type affiliations of volcanic exhalative ores. *Australas. Inst. Min. Metall. Monogr.* **1990**, *14*, 101–108.
9. Zharikov, V.A.; Pertsev, N.N.; Rusinov, V.L.; Callegari, E.; Fettes, D.J. Metasomatism and metasomatic rocks. In *A Classification of Metamorphic Rocks and Glossary of Terms. Recommendations of the International Union of Geological Sciences Subcommittee on the Systematics of Metamorphic Rocks*; IUGS: Paris, France, 2007; p. 17.
10. Roden, M.F.; Murthy, V.R. Mantle metasomatism. *Annu. Rev. Earth Planet. Sci.* **1985**, *13*, 269–296. [[CrossRef](#)]
11. Ferry, J.M.; Dipple, G.M. Fluid flow, mineral reactions, and metasomatism. *Geology* **1991**, *19*, 211–214. [[CrossRef](#)]
12. Stanley, C.R.; Madeisky, H.E. Lithogeochemical exploration for hydrothermal ore deposits using Pearce element ratio analysis. In *Alteration and Alteration Processes Associated with Ore-Forming Systems, Geological Association of Canada, Short Course Notes*; Lentz, D.R., Ed.; GAC: Guangzhou, China, 1994; Volume 11, pp. 193–211.
13. Gibson, H.L.; Allen, R.L.; Riverin, G.; Lane, T.E. The VMS model: Advances and application to exploration targeting. *Proc. Explor.* **2007**, *7*, 713–730.
14. Mathieu, L.; Bouchard, R.-A.; Pearson, V.; Daigneault, R. The Coulon deposit: Quantifying alteration in volcanogenic massive sulphide systems modified by amphibolite-facies metamorphism. *Can. J. Earth Sci.* **2016**, *53*, 1443–1457. [[CrossRef](#)]
15. Mathieu, L. Quantifying hydrothermal alteration with normative minerals and other chemical tools at the Beattie Syenite, Abitibi greenstone belt, Canada. *Geochem. Explor. Environ. Anal.* **2016**, *16*, 233–244. [[CrossRef](#)]
16. Kishida, A.; Kerrich, R. Hydrothermal alteration zoning and gold concentration at the Kerr-Addison Archean lode gold deposit, Kirkland Lake, Ontario. *Econ. Geol.* **1987**, *82*, 649–690. [[CrossRef](#)]
17. Piché, M.; Jébrak, M. Normative minerals and alteration indices developed for mineral exploration. *J. Geochem. Explor.* **2004**, *82*, 59–77. [[CrossRef](#)]
18. MacLean, W.H.; Barrett, T.J. Lithogeochemical techniques using immobile elements. *J. Geochem. Explor.* **1993**, *48*, 109–133. [[CrossRef](#)]
19. Gifkins, C.C.; Herrmann, W.; Large, R.R. *Altered Volcanic Rocks: A Guide to Description and Interpretation*; Centre for Ore Deposit Research, University of Tasmania: Hobart, Australia, 2005.
20. Simmons, S.F.; Christenson, B.W. Origins of calcite in a boiling geothermal system. *Am. J. Sci.* **1994**, *294*, 361–400. [[CrossRef](#)]
21. Guilbert, J.M.; Park, C.F., Jr. *The Geology of Ore Deposits, Freeman and Company*; W.H. Freeman and Co.: New York, NY, USA, 1986.



22. Lawley, C.J.M.; Dubé, B.; Mercier-Langevin, P.; Kjarsgaard, B.; Knight, R.; Vaillancourt, D. Defining and mapping hydrothermal footprints at the BIF-hosted Meliadine gold district, Nunavut, Canada. *J. Geochem. Explor.* **2015**, *155*, 33–55. [[CrossRef](#)]
23. Colvine, A.C. *Archean Lode Gold Deposits in Ontario*; OGS Miscellaneous Paper 139; Ontario Ministry of Northern Development and Mines: Greater Sudbury, ON, Canada, 1988; Volume 139, ISBN 077294105X.
24. Leitch, C.H.B.; Lentz, D.R. The Gresens approach to mass balance constrains of the alteration systems: Methods, pitfalls, examples. In *Alteration and Alteration Processes Associated with Ore-Forming Systems*; Lentz, D.R., Ed.; Geological Association of Canada: St. John's, NL, Canada, 1994; Volume 11, pp. 161–192.
25. Barrett, T.J.; MacLean, W.H. Chemostratigraphy and hydrothermal alteration in exploration for VHMS deposits in greenstones and younger volcanic rocks. In *Alteration and Alteration Processes Associated with Ore-Forming Systems*; Lentz, D.R., Ed.; Geological Association of Canada: St. John's, NL, Canada, 1994; Volume 11, pp. 433–465.
26. Large, R.R.; Gemmill, J.B.; Paulick, H.; Huston, D.L. The alteration box plot: A simple approach to understanding the relationship between alteration mineralogy and lithochemistry associated with volcanic-hosted massive sulfide deposits. *Econ. Geol.* **2001**, *96*, 957–971. [[CrossRef](#)]
27. Embley, R.W.; Jonasson, I.R.; Perfit, M.R.; Franklin, J.M.; Tivey, M.A.; Malahoff, A.; Smith, M.F.; Francis, T.J.G. Submersible investigation of an extinct hydrothermal system on the Galapagos Ridge; sulfide mounds, stockwork zone, and differentiated lavas. *Can. Mineral.* **1988**, *26*, 517–539.
28. Witt, W.K. Porphyry intrusions and albitites in the Bardoc-Kalgoorlie area, Western Australia, and their role in Archean epigenetic gold mineralization. *Can. J. Earth Sci.* **1992**, *29*, 1609–1622. [[CrossRef](#)]
29. Sangster, D.F. The role of dense brines in the formation of vent-distal sedimentary-exhalative (SEDEX) lead-zinc deposits: Field and laboratory evidence. *Miner. Depos.* **2002**, *37*, 149–157. [[CrossRef](#)]
30. Levesque, G. Duality of magmatism at Kirkland Lake, Ontario, Canada. Master's Thesis, University of Ottawa, Ottawa, ON, Canada, 1994.
31. Dominy, S.C. Sampling: A critical component to gold mining project evaluation. *Proj. Eval. Conf. Melb. Aust.* **2007**, *23*, 89–96.
32. Sarbas, B.; Nohl, U. The GEOROC database as part of a growing geoinformatics network. In *Geoinformatics Conference*; GSA: Washington, DC, USA, 2008.
33. Zheng, Y.C.; Gu, L.; Tang, X.; Wu, C.; Li, C.; Liu, S. Geology and geochemistry of highly metamorphosed footwall alteration zones in the Hongtoushan volcanogenic massive sulfide deposit, Liaoning Province, China. *Resour. Geol.* **2011**, *61*, 113–139. [[CrossRef](#)]
34. Allard, G.O. *Doré Lake Complex and Its Importance to Chibougamau Geology and Metallogeny*; MERN Report DP-386; Ministère des richesses naturelles: Québec, QC, Canada, 1976.
35. Guha, J. Hydrothermal systems and correlations of mineral deposits in the Chibougamau mining district—an overview. In *Chibougamau, Stratigraphy and Mineralization*; Guha, J., Chown, E., Eds.; Canadian Institute of Mining and Metallurgy: Westmount, QC, Canada, 1984; Volume 34, pp. 517–534.
36. Magnan, M.; Pilote, P.; Daigneault, R. *Minéralisations et Altérations à La MINE Copper Rand, Chibougamau*; MERN Report ET-98-01; Ministère de l'Énergie et des Ressources Naturelles: Québec, QC, Canada, 1999.
37. Jeffrey, W.G. The Geology of the Campbell Chibougamau Mine. Ph.D. Thesis, McGill University, Montreal, QC, Canada, 1959.
38. Pilote, P. Le camp minier de Chibougamau et le parautochtone grenvillien: Métallogénie, métamorphisme et aspects structuraux. In *Livret-Guide D'excursion B1*; Joined Annual Meeting; Geological Association of Canada—Mineralogical Association of Canada (GAC-MAC): Montreal, QC, Canada, 2006; p. 138.
39. Warren, R.G.; Shaw, R.D. Volcanogenic Cu-Pb-Zn bodies in granulites of the central Arunta Block, central Australia. *J. Metamorph. Geol.* **1985**, *3*, 481–499. [[CrossRef](#)]
40. Ravenelle, J.-F.; Dubé, B.; Malo, M.; McNicoll, V.; Nadeau, I.; Simoneau, J. *Insights on the Geology of the World-Class Roberto Gold Deposit, Éléonore property, James Bay Area, Quebec*; Current Research 2010-1; Geological Survey of Canada: Ottawa, ON, Canada, 2010; ISBN 1100145885.
41. Ravenelle, J.-F. Amphibolite Facies Gold Mineralization: An Exemple from the Roberto Deposit, Eleonore Property, James Bay, Quebec. Ph.D. Thesis, Université du Québec, Institut National de la Recherche Scientifique, Montreal, QC, Canada, 2013.

42. Fontaine, A.; Dubé, B.; Malo, M.; McNicoll, V.J.; Brisson, T.; Doucet, D.; Goutier, J. Geology of the metamorphosed Roberto gold deposit (Éléonore Mine), James Bay region, Quebec: Diversity of mineralization styles in a polyphase tectonometamorphic setting. In *Targeted Geoscience Initiative 4: Contributions to the Understanding of Precambrian Lode Gold Deposits and Implications for Exploration*; Dubé, B., Mercier-Langevin, P., Eds.; Geological Survey of Canada: Québec, QC, Canada, 2015; pp. 209–227.
43. Mercier-Langevin, P. Les minéralisations aurifères au sein de la tonalite de La Grande-Sud, Baie-James, Québec. Master's Thesis, Université du Québec à Chicoutimi, Chicoutimi, QC, Canada, 2000.
44. Mercier-Langevin, P.; Daigneault, R.; Goutier, J.; Dion, C.; Archer, P. Geology of the Archean intrusion-hosted La-Grande-Sud Au-Cu prospect, La Grande Subprovince, James Bay region, Quebec. *Econ. Geol.* **2012**, *107*, 935–962. [[CrossRef](#)]
45. MacLean, W.H.; Kranidiotis, P. Immobile elements as monitors of mass transfer in hydrothermal alteration; Phelps Dodge massive sulfide deposit, Matagami, Quebec. *Econ. Geol.* **1987**, *82*, 951–962. [[CrossRef](#)]
46. Ishikawa, Y.; Sawaguchi, T.; Iwaya, S.; Horiuchi, M. Delineation of prospecting targets for Kuroko deposits based on modes of volcanism of underlying dacite and alteration halos. *Min. Geol.* **1976**, *26*, 105–117.
47. Hughes, C.J. Spilites, keratophyres, and the igneous spectrum. *Geol. Mag.* **1972**, *109*, 513–527. [[CrossRef](#)]
48. Barth, T.F.W. Principles of classification and norm calculations of metamorphic rocks. *J. Geol.* **1959**, *67*, 135–152. [[CrossRef](#)]
49. Riverin, G.; Hodgson, C.J. Wall-rock alteration at the Millenbach Cu-Zn mine, Noranda, Quebec. *Econ. Geol.* **1980**, *75*, 424–444. [[CrossRef](#)]
50. Herrmann, W.; Berry, R.F. MINSQ—a least squares spreadsheet method for calculating mineral proportions from whole rock major element analyses. *Geochem. Explor. Environ. Anal.* **2002**, *2*, 361–368. [[CrossRef](#)]
51. Trépanier, S.; Mathieu, L.; Daigneault, R. CONSONORM-LG: New normative minerals and alteration indexes for low-grade metamorphic rocks. *Econ. Geol.* **2015**, *110*, 2127–2138. [[CrossRef](#)]
52. Mathieu, L.; Trépanier, S.; Daigneault, R. CONSONORM\_HG: A new method of norm calculation for mid-to high-grade metamorphic rocks. *J. Metamorph. Geol.* **2016**, *34*, 1–15. [[CrossRef](#)]
53. Middlemost, E.A.K. Iron oxidation ratios, norms and the classification of volcanic rocks. *Chem. Geol.* **1989**, *77*, 19–26. [[CrossRef](#)]
54. Le Maitre, R.W. The chemical variability of some common igneous rocks. *J. Petrol.* **1976**, *17*, 589–598. [[CrossRef](#)]
55. Warren, R.G. Metamorphic and tectonic evolution of granulites, Arunta Block, central Australia. *Nature* **1983**, *305*, 300–303. [[CrossRef](#)]
56. Groves, D.I.; Goldfarb, R.J.; Gebre-Mariam, M.; Hagemann, S.G.; Robert, F. Orogenic gold deposits: A proposed classification in the context of their crustal distribution and relationship to other gold deposit types. *Ore Geol. Rev.* **1998**, *13*, 7–27. [[CrossRef](#)]
57. Saeki, Y.; Date, J. Computer application to the alteration data of the footwall dacite lava at the Ezuri Kuroko deposits, Akita prefecture. *Min. Geol.* **1980**, *30*, 241–250.
58. Gresens, R.L. Composition-volume relationships of metasomatism. *Chem. Geol.* **1967**, *2*, 47–65. [[CrossRef](#)]
59. Babcock, R.S. Computational models of metasomatic processes. *Lithos* **1973**, *6*, 279–290. [[CrossRef](#)]
60. Brimhall, G.H.; Dietrich, W.E. Constitutive mass balance relations between chemical composition, volume, density, porosity, and strain in metasomatic hydrochemical systems: Results on weathering and pedogenesis. *Geochim. Cosmochim. Acta* **1987**, *51*, 567–587. [[CrossRef](#)]
61. Piercey, S.J. Modern analytical facilities 2. A review of quality assurance and quality control (QA/QC) procedures for lithochemical data. *Geosci. Can.* **2014**, *41*, 75–88. [[CrossRef](#)]
62. Trépanier, S.; Mathieu, L.; Daigneault, R.; Faure, S. Precursors predicted by artificial neural networks for mass balance calculations: Quantifying hydrothermal alteration in volcanic rocks. *Comput. Geosci.* **2016**, *89*, 32–43. [[CrossRef](#)]
63. Pearce, J.A.; Norry, M.J. Petrogenetic implications of Ti, Zr, Y, and Nb variations in volcanic rocks. *Contrib. Mineral. Petrol.* **1979**, *69*, 33–47. [[CrossRef](#)]
64. MacLean, W.H. Rare earth element mobility at constant inter-REE ratios in the alteration zone at the Phelps Dodge massive sulphide deposit, Matagami, Quebec. *Miner. Depos.* **1988**, *23*, 231–238. [[CrossRef](#)]
65. Rubin, J.N.; Henry, C.D.; Price, J.G. The mobility of zirconium and other “immobile” elements during hydrothermal alteration. *Chem. Geol.* **1993**, *110*, 29–47. [[CrossRef](#)]

66. Grant, J.A. Isocon analysis: A brief review of the method and applications. *Phys. Chem. Earth Parts A/B/C* **2005**, *30*, 997–1004. [[CrossRef](#)]
67. Grant, M. Étude du Métamorphisme et de la Distribution Verticale Des Teneurs en Au, As et Sb à la mine Sigma, Val-d'Or, Québec/Study of Metamorphism and Vertical Distribution of Au, As and Sb Grades at the Sigma mine, Val-d'Or, Québec. Master's Thesis, École Polytechnique de Montréal, Montreal, QC, Canada, 1986.
68. Leith, C.K.; Mead, W.J. *Metamorphic Geology*; Henry Holt: New York, NY, USA, 1915.
69. Goldich, S.S. A study in rock-weathering. *J. Geol.* **1938**, *46*, 17–58. [[CrossRef](#)]
70. Akella, J. Calculation of material transport in some metasomatic processes. *Neues Jahrb. Mineral. Abh.* **1966**, *104*, 316–329.
71. Krauskopf, K.B. *Introduction to Geochemistry*; McGraw-Hill: New York, NY, USA, 1979; ISBN 0070354472.
72. Finlow-Bates, T.; Stumpf, E.F. The behaviour of so-called immobile elements in hydrothermally altered rocks associated with volcanogenic submarine-exhalative ore deposits. *Miner. Depos.* **1981**, *16*, 319–328. [[CrossRef](#)]
73. Kranidiotis, P.; MacLean, W.H. Systematics of chlorite alteration at the Phelps Dodge massive sulfide deposit, Matagami, Quebec. *Econ. Geol.* **1987**, *82*, 1898–1911. [[CrossRef](#)]
74. Barrett, T.J.; MacLean, W.H. Chemical, mass, and oxygen isotope changes during extreme hydrothermal alteration of an Archean rhyolite, Noranda, Quebec. *Econ. Geol.* **1991**, *86*, 406–414. [[CrossRef](#)]
75. Barrett, T.J.; Cattalani, S.; Chartrand, F.; Jones, P. Massive sulfide deposits of the Noranda area, Quebec. II. The Aldermac mine. *Can. J. Earth Sci.* **1991**, *28*, 1301–1327. [[CrossRef](#)]
76. Barrett, T.J.; MacLean, W.H.; Cattalani, S.; Hoy, L.; Riverin, G. Massive sulfide deposits of the Noranda area, Quebec. III. The Ansil mine. *Can. J. Earth Sci.* **1991**, *28*, 1699–1730. [[CrossRef](#)]
77. Baumgartner, L.P.; Olsen, S.N. A least-squares approach to mass transport calculations using the isocon method. *Econ. Geol.* **1995**, *90*, 1261–1270. [[CrossRef](#)]
78. Shriver, N.A.; MacLean, W.H. Mass, volume and chemical changes in the alteration zone at the Norbec mine, Noranda, Quebec. *Miner. Depos.* **1993**, *28*, 157–166. [[CrossRef](#)]
79. Coggon, R.M.; Teagle, D.A.H.; Harris, M.; Davidson, G.J.; Alt, J.C.; Brewer, T.S. Hydrothermal contributions to global biogeochemical cycles: Insights from the Macquarie Island ophiolite. *Lithos* **2016**, *264*, 329–347. [[CrossRef](#)]
80. Tomkins, A.G.; Mavrogenes, J.A. Mobilization of gold as a polymetallic melt during pelite anatexis at the Challenger deposit, South Australia: A metamorphosed Archean gold deposit. *Econ. Geol.* **2002**, *97*, 1249–1271. [[CrossRef](#)]
81. Franklin, J.M.; Kasarda, J.; Poulsen, K.H. Petrology and chemistry of the alteration zone of the Mattabi massive sulfide deposit. *Econ. Geol.* **1975**, *70*, 63–79. [[CrossRef](#)]
82. McQueen, K.G. Ore deposit types and their primary expressions. In *Regolith Expression of Australian Ore Systems: A Compilation of Exploration Case Histories With Conceptual Dispersion, Process and Exploration Models*; Butt, C.R.M., Robertson, I.D.M., Scott, K.M., Cornelius, M., Eds.; Cooperative Research Centre for Landscape Environments and Mineral Exploration: Millaa Millaa, Australia, 2005; pp. 1–14.
83. Gaillard, N.; Williams-Jones, A.E.; Clark, J.R.; Lypaczewski, P.; Salvi, S.; Perrouy, S.; Piette-Lauzière, N.; Guilmette, C.; Linnen, R.L. Mica composition as a vector to gold mineralization: Deciphering hydrothermal and metamorphic effects in the Malartic District, Québec. *Ore Geol. Rev.* **2018**, 789–820. [[CrossRef](#)]
84. Nash, J.T. *Fluid-Inclusion Petrology-Data from Porphyry Copper Deposits and Applications to Exploration*; Professional Paper 907-D; U.S. Geological Survey: Reston, VA, USA, 1976.
85. Brauhart, C.W.; Huston, D.L.; Andrew, A.S. Oxygen isotope mapping in the Panorama VMS district, Pilbara Craton, Western Australia: Applications to estimating temperatures of alteration and to exploration. *Miner. Depos.* **2000**, *35*, 727–740. [[CrossRef](#)]
86. Beaudoin, G.; Pitre, D. Stable isotope geochemistry of the Archean Val-d'Or (Canada) orogenic gold vein field. *Miner. Depos.* **2005**, *40*, 59–75. [[CrossRef](#)]
87. Pearce, T.H. A contribution to the theory of variation diagrams. *Contrib. Mineral. Petrol.* **1968**, *19*, 142–157. [[CrossRef](#)]
88. Davis, L. *Handbook of Genetic Algorithms*; Van Nostrand Reinhold: New York, NY, USA, 1991.

